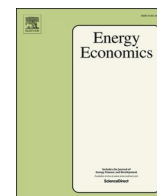


Risk network of global energy markets

Gazi Salah Uddin, Tianqi Luo, Muhammad Yahya, Ranadeva Jayasekera, Md Lutfur Rahman, Yarema Okhrin

Angaben zur Veröffentlichung / Publication details:

Uddin, Gazi Salah, Tianqi Luo, Muhammad Yahya, Ranadeva Jayasekera, Md Lutfur Rahman, and Yarema Okhrin. 2023. "Risk network of global energy markets." *Energy Economics* 125 (July): 106882. <https://doi.org/10.1016/j.eneco.2023.106882>.



Risk network of global energy markets

Gazi Salah Uddin^a, Tianqi Luo^b, Muhammad Yahya^{c,*}, Ranadeva Jayasekera^{b,d}, Md Lutfur Rahman^e, Yarema Okhrin^f

^a Department of Management and Engineering, Linköping University, Linköping, Sweden

^b Trinity Business School, Trinity College Dublin, Ireland

^c School of Economics and Business, Norwegian University of Life Sciences, Ås, Norway

^d Faculty of Business and Administration, Vilnius University, Vilnius, Lithuania

^e Newcastle Business School, The University of Newcastle, Australia

^f Faculty of Business and Economics, University of Augsburg, Germany

ARTICLE INFO

JEL classifications:

C32

C58

G11

G32

Q49

Keywords:

Energy companies

Systemic risk

Risk spillover

High-dimensional network

ABSTRACT

This study evaluates extreme uncertainty connectedness among top global energy firms. The sample comprises of 68 firms from four energy-related subsectors (oil & gas, oil & gas related equipment and services, multiline utilities, and renewable energy). To provide an overview of tail connectedness, we construct a high-dimensional network between firms by utilizing a generalized error decomposition and a sparse vector autoregression framework with a latent common factor. Our empirical results indicate that between the four subsectors, the renewable energy subsector exhibits the highest uncertainty transmission to other underlying subsectors, primarily credited to an increased within-subsector idiosyncratic uncertainty before the COVID-19 crisis. After the burst of the COVID-19 pandemic, due to the higher connectedness, the role of the renewable energy companies in the spillover network is further intensified. The uncertainty connectedness demonstrates a time-varying trait. While the oil and gas subsector exhibits greater long-term linkages with the oil and gas related equipment and services subsector, the long-run dynamics exhibit a lower interconnectedness as compared to the short-run. Finally, there is an increased connectedness among companies operating in the same subsector with similar size, attributing to similarity and competition.

1. Introduction

The management of systemic risk and risk contagion has become a top priority for policymakers, particularly after the global financial crisis. A risk becomes 'systemic' when there is a potential that a distress condition in one institution or a group of institutions can exert a negative externality on the entire system or economy (Kerste et al., 2015). A vast literature focuses on financial sector's systemic uncertainty (Silva et al., 2017). However, despite a significant correlation across energy companies' stock prices and their co-movement with the aggregate energy sector and overall stock market (see Appendix Table A1), the nature and extent of risk dependence or spillover among them are still under-researched. This is potentially due to the conventional belief that energy companies do not pose a significant systemic risk for their peer companies or the entire energy system (Zhu et al., 2020). We, however, argue that distress conditions in large energy companies (for example,

losses in firm values in response to a shock reflected in stock prices) can have a significant negative impact on other energy companies or the sector primarily due to their counterparty relationships. Therefore, it is essential to evaluate the nature of systemic uncertainty in the energy sector (Antonakakis et al., 2018; Kerste et al., 2015). The main aim of this study is to evaluate uncertainty connectedness and spillover among the top energy companies across the globe.

Theoretically, risk spillover between global energy companies may arise from several sources. First, energy companies' stock prices are likely to show a strong correlation as energy prices across countries are associated to international benchmark energy prices. Further, energy company outputs are typically homogenous (Sadorsky, 2001). Therefore, they are expected to exhibit a consistent response to energy price fluctuations and other geopolitical issues. For example, between July 2014 to December 2015, financial loss arising from the oil price decline caused 35 oil firms to apply for bankruptcy protection with a total debt

* Corresponding author.

E-mail addresses: gazi.salah.uddin@liu.se (G.S. Uddin), luot@tcd.ie (T. Luo), muhammad.yahya@nmbu.no (M. Yahya), jayasekr@tcd.ie (R. Jayasekera), Mdlutfur.Rahman@newcastle.edu.au (M.L. Rahman).

<https://doi.org/10.1016/j.eneeco.2023.106882>

Received 8 June 2022; Received in revised form 8 June 2023; Accepted 15 July 2023

Available online 18 July 2023

0140-9883/© 2023 The Author(s). Published by Elsevier B.V. This is an open access article under the CC BY license (<http://creativecommons.org/licenses/by/4.0/>).

of US\$18 billion (Natalia et al., 2018). Energy companies' fragility to energy price volatility is further amplified due to their highly leveraged and capital-intensive nature (Domanski et al., 2015; Zhu et al., 2020).

Second, due to high energy market integration (Zhu et al., 2020), large energy corporations are involved in a complicated relationship among themselves as suppliers, customers, and partners (see Appendix Table A2). These phenomena provide an important channel of financial contagion across energy companies. Related literature shows that the overall uncertainty spillover between energy firms is higher than that is observed in other sectors (Kerste et al., 2015; Natalia et al., 2018).

Third, energy derivatives, such as futures and options of gas, oil, and ultra-low-sulfur diesel (ULSD)¹ commodities are among the most widely traded financial contracts in the derivative markets (Natalia et al., 2018). Since energy firms are standard contributors to these derivative markets, they can spillover the risk of price shocks arising from speculation in the energy derivative markets.

Although there is a reasonably big literature on the dynamics of the global energy markets,² the risk spillover between energy companies has received less attention from researchers. Among the very few studies, Ewing et al. (2002) show significant and persistent volatility spillover between oil and gas companies, and Wen et al. (2014) evaluate the dependence among Chinese energy companies in return and volatility panels. Examining extreme risk spillover, Zhu et al. (2020) find that business complexity and geographic location (not firm size) are important drivers of the spillover between the energy companies. Natalia et al. (2018) find that energy firms have higher overall uncertainty spillover than stock markets, banks, exchange rates, or credit spread. Likewise, Kerste et al. (2015) show that linkages between distressed energy companies are the highest compared to those in other sectors (such as banks, insurance, construction, food). Based on textual risk disclosure data, Li et al. (2020) constructs a risk network of energy companies and find that oil and gas companies have the most crucial role in the network. However, none of the above studies has (i) examined risk connectedness using a high-dimensional network in energy firms; (ii) extracted idiosyncratic risk connectedness caused by the systematic factors, such as energy price, market volatility, and exogenous crisis (i. e., COVID-19 pandemic), etc.; (iii) considered an aggregated measure of systemic risk combining both bidirectional risk spillover as well as firm-specific idiosyncratic risk. The current study fills up this gap.

This paper makes both contextual and methodological contributions to the literature. First, the studies concentrating on risk spillover in the energy sector typically rely on energy indices (Singh et al., 2019) or aggregate energy company indices (Wen et al., 2014). Although few researchers explore risk spillover across energy companies, they mostly focus only on a small set of oil and gas producing companies (Kerste et al., 2015; Zhu et al., 2020; Natalia et al., 2018). We, therefore, contribute by using a large sample of 68 firms from four energy subsectors [Oil & Gas (OGC), Oil & Gas Related Equipment and Services (OGES), Multiline Utilities (MU), Renewable Energy (RE)]. To our best knowledge, this study is the first to provide evidence on risk dependence in all energy subsectors. We contend that aggregate analysis cannot capture heterogeneity in firm-level risk spillover. For instance, in the renewable energy subsector, systemic importance of a wind turbine company and a grain power company may be different. Although the

energy sector is vulnerable to exogenous shocks (such as oil prices changes) resulting in sector wide connectedness, it is important to understand firm-level idiosyncratic risk contagion. Further, concentrating only on the oil and gas subsector provides a partial picture of risk spillover in the energy sector.³ For example, the renewable energy subsector is becoming systemically more important as governments worldwide are pushing forward various regulations for a transition from conventional fossil fuels to renewable energy sources. Our granular study, therefore, aims to assist energy company managers, investors and policy makers by providing novel evidence of risk spillover across energy companies and subsectors (policy implications of our results are discussed in more details later in this section).

Second, we use a novel approach to estimate risk correlation and risk spillover between energy companies. Specifically, we firstly estimate conditional volatility and value-at-risk (VaR) for each energy company. We select the best model⁴ from various combinations of generalized autoregressive conditional heteroskedasticity (GARCH) model specifications and distributional assumptions of residuals.⁵ Then, we regard the risk connectedness between energy companies as a directional network linkage and construct a high-dimensional topological network. To measure risk connectedness, we estimate a vector auto-regression model with common factors (VAR-CF) suggested by Miao et al. (2022). Then, following an extended Diebold and Yilmaz (2014, DY afterward) framework, risk connectedness between each pair of companies is estimated by a generalized variance decomposition. While synthesizing the interdependence of a large sample of stock prices is a difficult job, our employed framework offers a parsimonious synthesis of data. The network analysis enables us to detect interconnectedness of volatility panels that provide information about uncertainty spillover networks. Finally, we use the risk decomposition of Das (2016) and Chen et al. (2019) to identify the companies and groups with risk contributions.

Third, although Li et al. (2020) constructs a risk network of energy companies, our paper is the first to estimate the high-dimensional network among global energy companies. We argue that the global energy sector comprising heterogeneous firms with varying degrees of front- and back-end operations is an excellent context for a high-dimensional network. Therefore, developing a high dimensional network constitutes an empirically feasible measure of tail-risk that accurately captures the dynamic contagion of companies' financial distress. As such, we contribute to this regard.

Finally, while prior papers (for instance, Kerste et al., 2015; Li et al., 2020; Natalia et al., 2018) mostly identify systemic significance of an energy firm or a sector by applying dependence or connectedness, we argue that the systemic risk contribution should not be analyzed without considering the idiosyncratic risk profile. In the literature of systemic uncertainty in the financial market, firm-specific idiosyncratic risk profile (typically estimated by VaR) is reported as a driver of risk spillover and is incorporated in the systemic risk modelling (see Adrian and Brunnermeier, 2016; Hautsch et al., 2015). Therefore, we measure systemic uncertainty by aggregating the connectedness with firm-specific idiosyncratic risk. This exercise enables us to portray the

¹ ULSD generally refers to diesel fuel with a sulfur content of <15 ppm (in the US) or <50 ppm (in the EU).

² The literature has focused on integration and interdependence of the global energy market (Ji and Fan, 2015, 2016; Bachmeier and Griffin, 2006; Jia et al., 2017), extreme uncertainty connectedness inside energy markets, and the linkage between energy and other markets (Fan et al., 2008; Du and He, 2015; Shahzad et al., 2018), volatility contagion from energy market to other markets (Masih et al., 2011; Luo and Qin, 2017; Natanelov et al., 2011), and the impacts of energy price on oil and gas companies (Hammoudeh et al., 2004; Elyasiani et al., 2011).

³ This is because oil and gas producing companies are only a segment of the entire energy sector. As of 31 December 2019, international oil and gas producing companies contributed only 54.22% of the total market capitalization of the global energy industry. The remaining was contributed by energy companies involving refining and marketing, equipment and services, pipelines, coal, and alternative energy production and distribution (Source: Refinitiv DataStream sectoral indices).

⁴ ARMA (1,1)-GJRARCH (3,3) model with Gaussian distribution.

⁵ We consider various combinations of ARMA (m,n) models [such as ARMA (0,0), ARMA(0,1), ARMA(1,0), and ARMA(1,1)], GARCH frameworks (GARCH, IGARCH, EGARCH, GJRARCH, TGARCH) and distributional assumptions (Normal, Student-T, and Skewed-T distribution)

complete picture of systemic uncertainty in the international energy market.

This paper reports several key findings. First, among the four subsectors, companies from the renewable energy subsector demonstrate the highest uncertainty contribution to the overall market, which is primarily attributed to the within sector uncertainty. A pairwise asymmetric effect indicates that in 2020–2021, the oil and gas related equipment and services subsector is a receiver of spillover risk, while the renewable energy subsector serve as a transmitter. Second, the long-term network of energy firms is dominated by the linkage between the oil and gas and oil and gas related equipment and services subsectors. Third, the connectedness deteriorates after a certain period with a special event, resulting in a lower value of long-term connectedness than short-term. Finally, the significant spillover risks are more often to occur between two firms with similar firm size and subsector, which could relate to the segment-wide competition and similarity, as discussed by Gong (2018).

Our results have important policy implications. Energy company managers may use the findings to mitigate risks of spillover from other companies in energy industry. The results can also help them understand the high dimensional dynamics of global energy companies. The findings can be useful for international portfolio managers that allocate their capital to energy-related companies.⁶ Further, the tools used in this paper may assist energy companies' managers to improve financial risk measurement and management. While the global energy sector is gradually transitioning from fossil-based energy to renewable energy sources, our findings about the uncertainty contribution of renewable energy firms can assist in understanding the capital market implications of this transition.

The rest of the paper is structured as follows. Section 2 provides the framework to measure idiosyncratic risk, connectedness, and systemic risk. In Section 3, we introduce the data sample and present preliminary statistics. Section 4 analyses empirical findings, and section 5 concludes the paper.

2. Methodology

This paper examines the risk spillover network among energy firms by a three-step approach. In the first step, we estimate volatility and idiosyncratic risk of each energy company, based on a GARCH model section procedure. The estimated results of volatility and idiosyncratic risk are respectively used as input data for the second and third steps. In the second step, we measure risk connectedness between energy companies as a directional network linkage and construct a high-dimensional topological network. To measure risk connectedness, we estimate a vector auto-regression model with common factor (abbreviated as VAR-CF model) suggested by Miao et al. (2022). Then following DY (2014) framework, risk connectedness between each pair of companies is estimated by a generalized variance decomposition. The network analysis enables us to detect interconnectedness of volatility panels that provide information about risk transmission channels. In the third step, we estimate systemic uncertainty by aggregating the interconnectedness with the firm-specific uncertainty. This method allows us to parsimoniously synthesize the interdependence of a large sample of stock prices into an aggregated value. Finally, by using the risk

decomposition of Das (2016) and Chen et al. (2019), we identify the companies and groups with relatively higher values of systemic risk contributions. In the full estimation procedure, we examine both long-run and short-run spillover risk among the four energy subsectors. Our three-step methodological approach is described below.

2.1. Firm-specific conditional volatility and idiosyncratic risk

In the first step, we utilize GARCH model to estimate latent volatility, which is the input data for the second step to calculate risk connectedness. We also use GARCH model to measure firm-specific idiosyncratic risk by estimating value-at-risk (VaR) for each energy company. To implement an accurate estimation of volatility and VaR, we use various settings in GARCH models. For variance specification, we include GARCH, IGARCH, EGARCH, and GJR-GARCH with different lag lengths of ARCH and GARCH terms. Similarly, for return specification, we include ARMA with different lag lengths of autoregressive and moving average terms. For the standardized residual of the return modelling, we test Normal, Student-T, and Skewed-T distribution. Based on the Akaike information criterion (AIC), the ARMA (1,1)-GJR-GARCH (3,3) framework with Gaussian distribution is the best-fitted model.⁷ The model is explained below:

Let $r_{i,t}$ correspond to a stochastic process of returns for the i_{th} series

$$r_{i,t} = \mu_i + \beta_0 r_{i,t-1} + u_{i,t} + \beta_1 u_{i,t-1} \quad (1)$$

where $u_{i,t} = \varepsilon_{i,t} \sigma_{i,t}$ are the residuals. The white noise process, $\varepsilon_{i,t} \sim i.i.d(0, 1)$ follows the Gaussian distribution. We model the latent volatility $\sigma_{i,t}$ with the GJR-GARCH (3,3) specification.

$$\sigma_{i,t}^2 = \alpha_0 + \sum_{p=1}^3 \alpha_p u_{i,t-p}^2 + \sum_{p=1}^3 \alpha_p^- S_{i,t-p}^- u_{i,t-p}^2 + \sum_{q=1}^3 \eta_q \sigma_{i,t-q}^2 \quad (2)$$

where $S_{i,t-p}^- = \begin{cases} 1, & \text{if } u_{i,t-p} < 0 \\ 0, & \text{otherwise} \end{cases}$, $\alpha_0 > 0$, $\alpha_m > 0$.

The idiosyncratic risk is measured by VaR, which can be estimated by a percentile (i.e. quantile) of the stochastic process of return.

$$VaR_{i,t} = -(\mu_i + \hat{\beta}_0 r_{i,t-1} + \hat{\beta}_1 \hat{u}_{i,t-1} + Z_q \hat{\sigma}_{i,t}) \quad (3)$$

where Z_q denotes the corresponding quantile of the Gaussian distribution in quantile level q . We use $q = 0.01$ to measure the extreme tail risk. Note $Z_{0.01}$ is in the left of the distribution and the quantile value is negative. We obtain positive series by adding a negative sign in eq.(3) for the convenience of our subsequent estimation and interpretation.

2.2. High-dimensional VAR with common factor (VAR-CF)

To measure risk connectedness in a high-dimensional panel, we utilize an improved version of DY (2014) framework. Consider a p -order vector autoregression (VAR) process with common factors (CFs),

$$Y_t = \sum_{k=1}^p A_k^0 Y_{t-k} + \Lambda^0 f_t^0 + u_t, t = 1, 2, \dots, T \quad (4)$$

where $Y_t = \{y_{1,t}, y_{2,t}, \dots, y_{N,t}\}'$ is the multivariate time series of volatility with N dimensions and A_k is a $N \times N$ autoregressive coefficient matrix. This framework allows for both the number of cross-sectional units N and the number of time periods T to pass to infinity. $\Lambda^0 =$

⁶ As we estimate systemic risk contribution and spillover risk of the individual companies and energy subsectors, this provides with information for devising portfolio strategies. Specifically, a higher or lower value of connectedness/spillover may indicate risk contagion or diversification respectively. As such, portfolio managers should rebalance their portfolios when two stocks show a high (low) degree of connectedness as this can increase (decrease) systemic risk and reduce (increase) diversification benefits. Overall, connectedness dynamics can help portfolio managers optimize their portfolios by minimizing potential losses from spillover risks.

⁷ While we rely on GARCH-based models, we acknowledge that stochastic volatility (SV) models could be used for volatility modelling in this paper. However, since we use the VAR-CF model with a rolling window estimation for 68 companies, using SV models for this large sample and alternative estimations would be extremely challenging. We, therefore, leave this for future research.

$(\lambda_1^0, \lambda_2^0, \dots, \lambda_N^0)'$ is an $N \times R^0$ factor loading matrix and f_t^0 is an R^0 dimensional vector of common factor. The latent factor structure, represented by $\Lambda^0 f_t^0$, captures systematic shocks which can intensify cross-sectional dependence. $u_t \equiv (u_{1,t}, u_{2,t}, \dots, u_{N,t})'$ is an N -dimensional vector of unobserved idiosyncratic errors. Throughout this paper, we use the superscript 0 to denote true values. The coefficients to be estimated are the A_k^0 , Λ^0 , and $F^0 \equiv (f_1^0, f_2^0, \dots, f_T^0)'$.

The model is reformulated in multivariate form as

$$\underbrace{\begin{bmatrix} Y_1' \\ \vdots \\ Y_T' \end{bmatrix}}_{\mathbf{Y}} = \underbrace{\begin{bmatrix} Y_0' & \dots & Y_{1-p}' \\ \vdots & \ddots & \vdots \\ Y_{T-1}' & \dots & Y_{T-p}' \end{bmatrix}}_{\mathbf{X}} \underbrace{\begin{bmatrix} A_1^0 \\ \vdots \\ A_p^0 \end{bmatrix}}_{\mathbf{B}^0} + \underbrace{\begin{bmatrix} f_1^0 \\ \vdots \\ f_T^0 \end{bmatrix}}_{\mathbf{F}^0} \underbrace{\begin{bmatrix} \lambda_1^0 \\ \vdots \\ \lambda_N^0 \end{bmatrix}}_{\Lambda^0} + \underbrace{\begin{bmatrix} u_1' \\ \vdots \\ u_T' \end{bmatrix}}_{\mathbf{U}} \quad (5)$$

where $\mathbf{Y} \in \mathbb{R}^{T \times N}$, $\mathbf{X} \in \mathbb{R}^{T \times Np}$, $\mathbf{B}^0 \in \mathbb{R}^{Np \times N}$ and $\mathbf{U} \in \mathbb{R}^{T \times N}$. Let $\Theta^0 \equiv \mathbf{F}^0 \Lambda^0$ denotes the common component matrix with low rank. Note that the principal component analysis on \mathbf{Y} cannot deliver a consistent estimate of the common factors because of the presence of $\mathbf{X}\mathbf{B}^0$. Therefore, the consistent common factors are obtained based on a hard singular value thresholding (SVT) and a singular value decomposition (SVD).

2.2.1. Estimation

To estimate the VAR-CF model, we follow the procedure of Miao et al. (2022) with three steps. The first step aims to obtain the initial estimates of Θ^0 , \mathbf{B}^0 and \mathbf{F}^0 . The coefficient matrix \mathbf{B}^0 is set to be sparse, which typically have a low density of none-zero connections.⁸

We apply an ℓ_1 -nuclear-norm regularized regression which estimates \mathbf{B}^0 and Θ^0 simultaneously,

$$(\hat{\mathbf{B}}, \hat{\Theta}) = \underset{(\mathbf{B}, \Theta)}{\operatorname{argmin}} \mathcal{L}(\mathbf{B}, \Theta) \quad (6)$$

$$\mathcal{L}(\mathbf{B}, \Theta) \equiv \frac{1}{2NT} \|\mathbf{Y} - \mathbf{X}\mathbf{B} - \Theta\|_F^2 + \frac{\gamma_1}{N} |\operatorname{vec}(\mathbf{B})|_1 + \frac{\gamma_2}{\sqrt{NT}} \|\Theta\|_* \quad (7)$$

where the γ_1 and γ_2 are tuning parameters. The selection of tuning parameters will be illustrated in section 2.2.2. For any matrix $\mathbf{A} = (a_{ij}) \in \mathbb{R}^{M \times N}$ the $\|\mathbf{A}\|_F = \left(\sum_{i,j} |a_{ij}|^2 \right)^{1/2}$ and $\|\mathbf{A}\|_* = \sum_{k=1}^{\min(N,M)} \psi_k(\mathbf{A})$, where $\psi_k(\mathbf{A})$ denotes the k th largest singular value of \mathbf{A} for $k = 1, \dots, \min(M, N)$. We define the norms ℓ_0 and ℓ_q ($q \geq 1$) of a vector \mathbf{v} as $|\mathbf{v}|_0 = \sum_{i=1}^N \mathbf{1}(v_i \neq 0)$ and $|\mathbf{v}|_q = \left(\sum_{i=1}^N |v_i|^q \right)^{1/q}$. The numerical solutions of

\mathbf{B} and Θ are obtained based on an expectation maximization (EM) type algorithm. We firstly fix \mathbf{B} and update the estimate of Θ (E-step), then fix Θ and update \mathbf{B} (M-step). It can be considered as a Lasso-type linear regression problem with many steps of iteration.

The number of factors R^0 can be estimated by SVT,

⁸ Note that sparseness for model selection is an approach that generates a small number of nonzero coefficients that are uniformly bounded away from zero at a certain rate. Since we use several systematic factors (see subsection 4.2 for the factor details), sparsity is used to shrink the parameter matrix and maintain the degree of freedom. This approach is commonly used in high-dimensional data modelling. Although using penalties in the likelihood function shrinks the coefficients, it does not reduce errors to zero. The sparse matrix in the VAR model provides a sparse solution, i.e., a set of estimated coefficients in which only a small number are non-zero. This helps us capture crucial relationships within the variables. Overall, sparsity improves predictive accuracy (Hastie et al., 2015).

$$\hat{R} = \sum_{i=1}^{N \wedge T} \mathbf{1} \left\{ \psi_i(\tilde{\Theta}) \geq \left(\gamma_2 \sqrt{NT} \|\tilde{\Theta}\|_{op} \right)^{1/2} \right\} \quad (8)$$

where $\psi_i(\tilde{\Theta})$ are the singular values of $\tilde{\Theta}$. The $\|\mathbf{A}\|_{op} = \psi_{\max}(\mathbf{A})$, i.e., the largest singular values of \mathbf{A} . Based on the SVD that $\tilde{\Theta} = \tilde{\mathbf{U}}\tilde{\mathbf{D}}\tilde{\mathbf{V}}'$, where $\tilde{\mathbf{D}} = \operatorname{diag}(\psi_1(\tilde{\Theta}), \dots, \psi_{N \wedge T}(\tilde{\Theta}))$, the initial estimates of \mathbf{F}^0 can be given by $\tilde{\mathbf{F}} = \sqrt{T}\tilde{\mathbf{U}}_{*,[R]}$.

The second step uses a plain Lasso to estimate the elements of the factor loadings and transition matrix. For each firm $i \in N$, we estimate a time series regression of $\mathbf{Y}_{*,i}$ on $(\mathbf{X}, \tilde{\mathbf{F}})$ by imposing an ℓ_1 -norm penalty on the coefficient of \mathbf{X} , by solving the minimization problem.

$$(\hat{\mathbf{B}}_{*,i}', \hat{\lambda}_i') = \underset{(\mathbf{v}', \lambda') \in \mathbb{R}^{Np \times R^0}}{\operatorname{argmin}} \frac{1}{2T} \|\mathbf{Y}_{*,i} - \mathbf{X}\mathbf{v} - \tilde{\mathbf{F}}\lambda\|_F^2 + \gamma_3 |\mathbf{v}|_1 \quad (9)$$

The estimators of transition matrix and factor loading are given by

$$\hat{\mathbf{B}} = (\hat{\mathbf{B}}_{*,1}, \dots, \hat{\mathbf{B}}_{*,N}) \text{ and } \hat{\Lambda} = (\hat{\lambda}_1, \dots, \hat{\lambda}_N)'. \text{ The } \gamma_3 \text{ is tuning parameter.}$$

Since the imposed penalties on the transition matrix introduce asymptotic bias into the estimator of the transition matrix, the third step applies a conservative Lasso which gives the initial zero coefficient estimates a second chance to be none-zero.

The third step is implemented by using a weight in the conservative Lasso minimization,

$$w_{ki} = \begin{cases} 1 & \text{if } |\hat{\mathbf{B}}_{ki}| < \alpha\gamma_4 \\ 0 & \text{if } |\hat{\mathbf{B}}_{ki}| \geq \alpha\gamma_4 \end{cases} \quad (10)$$

where $k \in [Np]$, $i \in [N]$, and $\alpha > 0$. Set $\hat{\mathbf{F}}^{(0)} = \tilde{\mathbf{F}}$. The γ_4 is tuning parameter. Then, for integer $\ell \geq 1$, update the transition matrix and factor loading by

$$(\hat{\mathbf{B}}_{*,i}^{(\ell)}, \hat{\lambda}_i^{(\ell)}) = \underset{(\mathbf{v}', \lambda') \in \mathbb{R}^{Np \times R}}{\operatorname{argmin}} \frac{1}{2T} \|\mathbf{Y}_{*,i} - \mathbf{X}\mathbf{v} - \hat{\mathbf{F}}^{(\ell-1)}\lambda\|_F^2 + \gamma_4 \sum_{k=1}^{Np} w_{ki} |v_k| \quad (11)$$

where v_k is the k th entry of \mathbf{v} , $i \in [N]$. Let $\hat{\mathbf{B}}^{(\ell)} = (\hat{\mathbf{B}}_{*,1}^{(\ell)}, \dots, \hat{\mathbf{B}}_{*,N}^{(\ell)})$. By using the SVD, the common factor is updated by $\mathbf{Y} - \mathbf{X}\hat{\mathbf{B}}^{(\ell)} = \hat{\mathbf{U}}^{(\ell)}\hat{\mathbf{D}}^{(\ell)}\hat{\mathbf{V}}^{(\ell)'} \text{ and } \hat{\mathbf{F}}^{(\ell)} = \sqrt{T}\hat{\mathbf{U}}_{*,[R]}^{(\ell)}$. Afterwards, set $\ell = \ell + 1$ and iterate the updating of transition matrix, factor loading, and common factor for a finite time ℓ^* . The final estimators are denoted by $\hat{\mathbf{B}} = \hat{\mathbf{B}}^{(\ell^*)}$, $\hat{\mathbf{F}} = \hat{\mathbf{F}}^{(\ell^*-1)}$, and $\hat{\Lambda} = \hat{\Lambda}^{(\ell^*)}$.

2.2.2. Tuning parameter selection

To estimate the VAR-CF model, the tuning parameters $\gamma_1, \gamma_2, \gamma_3, \gamma_4$ need to be selected. We firstly select γ_1, γ_3 , and γ_4 by a 5-fold cross validation method. Specifically, let $\gamma = (\gamma_1, \gamma_3, \gamma_4)'$, and the full period is divided into 5 parts: $T_1, \dots, T_5 \in [T]$. For $k = 1, \dots, 5$, we fit the VAR-CF model by using a data set that excludes the k th fold data, and obtain the estimators of transition matrix, factor loading, and common factor. For a $T \times R$ full rank matrix \mathbf{F} with $T > R$, $\mathbb{M}_{\mathbf{F}} = \mathbf{I}_T - \mathbf{F}(\mathbf{F}'\mathbf{F})^{-1}\mathbf{F}'$ where \mathbf{I}_T is the $T \times T$ identity matrix. The sum of squared prediction errors is calculated by $cv(\gamma, k) = \operatorname{tr} \left[\left(\mathbf{Y}_{T_k, * - \mathbf{X}_{T_k, *} \hat{\mathbf{B}}^{(\gamma, k)} \right) \mathbb{M}_{\hat{\Lambda}^{(\gamma, k)}} \left(\mathbf{Y}_{T_k, * - \mathbf{X}_{T_k, *} \hat{\mathbf{B}}^{(\gamma, k)} \right)' \right]$. Then we summarize $CV(\gamma) = \sum_{k=1}^5 cv(\gamma, k)$, and select $\gamma^* = \operatorname{argmin}_{\gamma} CV(\gamma)$. The γ_2 is based on the simulation of \mathbf{U} . Suppose the entries of \mathbf{U} follow Gaussian distribution with a zero mean and standard deviation $\hat{\sigma}_u$. Then the $\gamma_2 = Q(\|\mathbf{U}\|_{op}, 0.95) / \sqrt{NT}$, where the $Q(x, \alpha)$ denotes the α th quantile of x .

2.3. Connectedness

We use the extended measure of connectedness to study the network relationship of “fears” among energy companies, where common factors are taken into account in the DY (2014) framework. The error variance of a firm could be caused by both common factors and other firms, i.e., $y_{i,t} = y_{i,t}^{(f)} + y_{i,t}^{(u)} \cdot y_{i,t}^{(u)}$ measures the idiosyncratic shock to firm i , i.e., $y_{i,t}^{(u)} = \sum_{j=0}^{\infty} \alpha_{iN}^{(u)}(j) u_{t-j}$. Given $u_t = C^{(u)} e_t^{(u)}$, $e_t^{(u)} = (\epsilon_{1,t}^{(u)}, \dots, \epsilon_{m,t}^{(u)})'$, where $\epsilon_{i,t}^{(u)}$ is i.i.d (0,1), and $C^{(u)}$ is an $N \times m$ identity matrix $y_{i,t}^{(u)} = \sum_{j=0}^{\infty} \alpha_{iN}^{(u)}(h) C^{(u)} e_{t-j}^{(u)}$. The covariance matrix $\Sigma_u = C^{(u)} C^{(u)'}$, and σ_{jj} is the j th diagonal entry of matrix Σ .

The $\alpha_{iN}^{(u)}(j) = (e_{1,p} \otimes e_{iN})' \phi^j (e_{1,p} \otimes I_N)$, where e_{ij} is the entry with rows and columns are indexed by i and j . And the ϕ^j is the j power of the

$$\phi = \begin{bmatrix} A_1^0 & A_2^0 & \dots & A_{p-1}^0 & A_p^0 \\ I_N & \mathbf{0} & \dots & \mathbf{0} & \mathbf{0} \\ \mathbf{0} & I_N & \dots & \mathbf{0} & \mathbf{0} \\ \vdots & \vdots & \ddots & \vdots & \vdots \\ \mathbf{0} & \mathbf{0} & \dots & I_N & \mathbf{0} \end{bmatrix} \quad (12)$$

The H-step-ahead generalized variance decomposition is utilized to generate the interconnectedness matrix $\theta^H = [\theta_{ij}^H]$, whose entries are the proportions of idiosyncratic error variance in i_{th} firm caused by a standard error of shock in j_{th} firm

$$\theta_{ij}^H = \frac{\sigma_{ij}^{-1} \sum_{h=0}^{H-1} (\alpha_{iN}^{(u)}(h) \Sigma_u e_{jN})^2}{\sum_{h=0}^{H-1} (\alpha_{iN}^{(u)}(h) \Sigma_u \alpha_{iN}^{(u)}(h)')} \quad (13)$$

The high value of θ_{ij}^H implies a strong risk interdependence between two firms, i.e., the shock of i_{th} firm would contribute to a relatively big response on the risk of j_{th} firm. Note that θ_{ij}^H could have unequal value with θ_{ji}^H , which is recognized as asymmetric effect between two firms and construct directional linkages between two nodes in the topological network of energy firms. Note that, we haven't adopted the normalization process of θ_{ij}^H that $\tilde{\theta}_{ij}^H = \theta_{ij}^H / \sum_{j=1}^N \theta_{ij}^H$ for two reasons. First, the normalization makes the sum value of connectedness of each output company to be 1. Second, observations of unnormalized connectedness contains more information about the time-varying network relationship and systemic risk contribution.

2.4. Systemic and spillover risk

Thus far (in the previous subsection), we have explained the methodologies related to risk connectedness measure in a high-dimensional panel [the extended DY (2014) framework and the VAR-CF model]. While this connectedness reflects systemic importance of an energy company or a sector, it does not capture firm-specific idiosyncratic risk profile. We, therefore, quantify the aggregated risk in a network (discussed below) following Das (2016) and Chen et al. (2019) and use value-at-risk (VaR) as compromise loading. This is theoretically intuitive. While previous studies focusing on risk spillover in the energy sector mostly ignore firms' idiosyncratic risk (for example, Kerste et al., 2015; Li et al., 2020; Natalia et al., 2018), we argue that the systemic risk contribution of a company should not be analyzed without considering its idiosyncratic risk profile. The literature of systemic risk in financial markets commonly reports firm-specific idiosyncratic risk profile (typically estimated by VaR) as a driver of risk spillover (see Adrian and Brunnermeier, 2016; Hautsch et al., 2015). Recent research also shows that US oil and gas companies' VaR contributes to their

systemic risk profile (Caporin et al., 2023). Therefore, we estimate systemic uncertainty by aggregating connectedness with firm-specific idiosyncratic risk.

To quantify the aggregated risk in a network, Das (2016) and Chen et al. (2019) provide the technique that aggregate an adjacency matrix with a compromise loading. In this paper, we use VaRs of firms as the compromise level. With the level of compromises $V = (VaR_1, VaR_2, \dots, VaR_N)^T$, we estimate risk scores as the measure of systemic risk by

$$S_{system}(V, \theta^H) = V^T \theta^H V \quad (14)$$

where S_{system} is the aggregated value of systemic risk. θ^H is the adjacency matrix obtained in the former subsection. Then by Euler's theorem,⁹ we decompose the aggregated S_{system} into firm-specific systemic risk contribution as

$$S_{system}(V, \theta^H) = \frac{1}{2} \left[\frac{\partial S}{\partial V_1} V_1 + \frac{\partial S}{\partial V_2} V_2 + \dots + \frac{\partial S}{\partial V_N} V_N \right] \quad (15)$$

where $\frac{\partial S}{\partial V_i} = \sum_{j=1}^N \theta_{ij}^H V_j + \theta_{ji}^H V_j$ is the risk increment that indicates changes in the aggregate network risk score S when the compromise score V_i changes. From the aggregated risk score, we decompose the risk contribution of each node from the systemic risk score by

$$D_i = \frac{1}{2} \frac{\partial S}{\partial V_i} V_i \quad (16)$$

From the aggregated risk score, we also induce risk spillover between each pair of series (i, j) , as

$$S_{ij} = V_i^T \theta_{ij}^H V_j \quad (17)$$

The risk spillover S_{ij} for each pair of series (i, j) combine the risk level of the source and target companies and the connection that indicates the interaction of risks. It is noteworthy that the $S_{system} = \sum_{i=1}^N \sum_{j=1}^N S_{ij}$, where N denotes the number of companies in this network. The θ_{ij}^H measures the proportion of idiosyncratic error variance in firm i caused by a standard error of shock in firm j . With the compromise loading of VaR, risk spillover S_{ij} measures the consequence of the idiosyncratic risk in firm i on the idiosyncratic risk in firm j . Compared with the connectedness θ_{ij}^H which was regarded as a measure of spillover, our model takes two new developments: (1) the source and channel of spillover are the idiosyncratic risk of each firm, (2) the spillover is calculated based on the daily idiosyncratic risk, where a price decrease (increase) of a source firm intensifies (alleviates) the spillover hazard for a target firm.

Given group M and N as import and export panels, the risk score that measures spillover from group N to M is specified as:

$$S_{MN} = V_M^T \theta_{MN}^H V_N \quad (18)$$

where V_M denotes the panel of idiosyncratic risks that belong to group M . θ_{MN}^H is the submatrix of adjacency matrix θ^H that indicate the shares of error variance in all series in Group N due to shocks of all series in Group M . Note that $S_{system} = \sum_{M=1}^G \sum_{N=1}^G S_{MN}$, where G denotes the number of groups.

3. Data and descriptive statistics

This paper utilizes daily stock price for the sample period ranging from December 31, 2011, to 11 November 2022 with 2835 daily observations for each timeseries. The sample period is determined pri-

⁹ Euler's theorem states that for a function $f(x)$, $x \in R^N$ is homogeneous of degree n and it may be written as $\frac{1}{n} \sum_{i=1}^N \frac{\partial f(x)}{\partial x_i} x_i$

Table 1
Descriptive statistics and stochastic properties.

	Oil & Gas (OGC)	Oil & Gas Related Equipment and Services (OGES)	Multiline Utilities (MU)	Renewable Energy (RE)
Mean (%)	0.007	−0.025	0.006	0.037
Standard Deviation (%)	2.031	2.471	1.658	3.603
Sharpe Ratio	−0.392	−0.351	−0.482	−0.216
Maximum (%)	16.571	19.902	13.179	25.948
Minimum (%)	−23.116	−28.986	−16.668	−25.909
Skewness	−0.700	−0.926	−0.651	0.076
Kurtosis	16.974	20.155	13.621	8.065
Jarque-Bera	45,255.273***	85,363.908***	29,225.853***	13,573.731***
Q (20)	68.127**	70.267*	83.488**	39.493
Q2 (20)	1204.085***	983.468***	1555.525***	382.395***
ARCH-LM (20)	557.523***	440.584***	535.085***	177.207***
ARCH-LM (residual)	11.399	10.391	9.241	19.583

Note. This table provides the stochastic properties of underlying companies by subsector-wise average. Jarque-Bera statistics denotes the normality test of [Jarque and Bera \(1987\)](#). Q (20) and Q2 (20) show the autocorrelation test statistics in returns and squared returns, respectively, by the Ljung-Box test. ARCH-LM (20) corresponds to the results of [Engle \(1982\)](#) test of ARCH effects in returns. ARCH-LM (residual) corresponds to the results of [Engle \(1982\)](#) test of ARCH effects in the standardized residuals of the GJR-GARCH model. ***, **, and *, respectively, suggest statistical significance at the 1%, 5%, and 10% level.

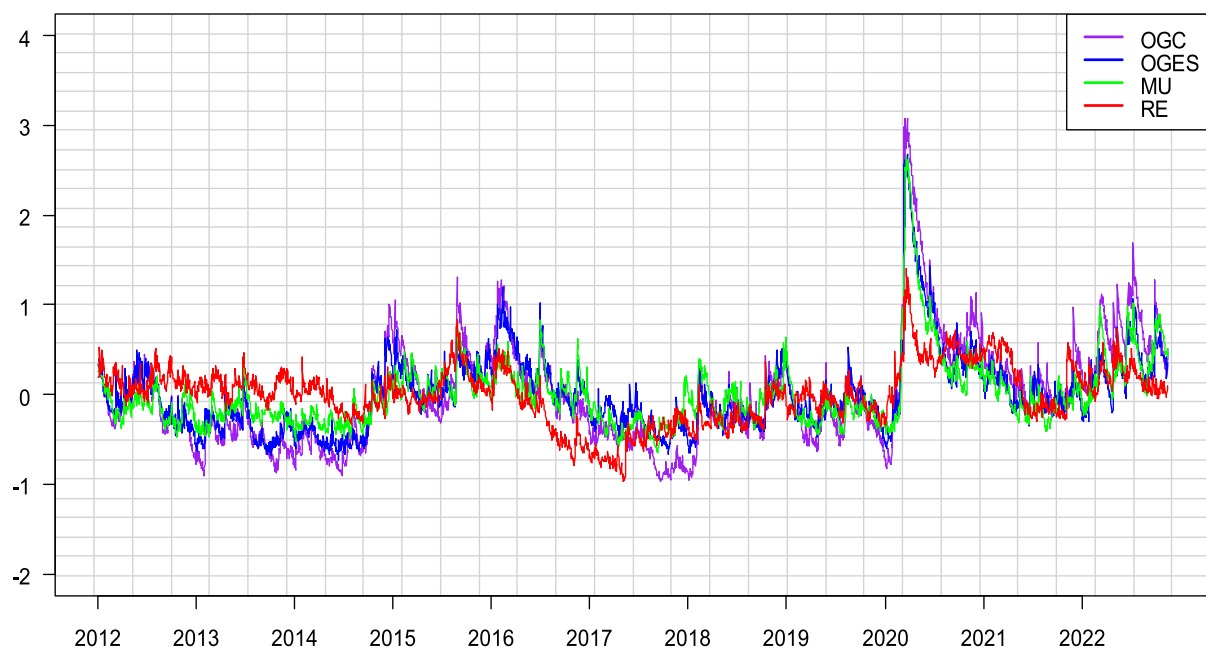


Fig. 1. Conditional variance of each energy subsector.

Note. This figure reports the daily log conditional variance standardized with zero mean value, averaged by energy subsectors. OGC: oil and gas; OGES: oil and gas related equipment and services; MU: multiline utilities, and RE: renewable energy. OGC, OGES, MU, and RE are respectively indicated by purple, blue, green, and red. Conditional variance for each firm is calculated by the ARMA (1,1)-GJR-GARCH (3,3) framework with Gaussian distribution. (For interpretation of the references to colour in this figure legend, the reader is referred to the web version of this article.)

marily by the data availability. The sample includes 17 firms from each energy subsector (oil and gas, oil and gas related equipment and services, multiline utilities and renewable energy) totaling 68 firms. We select firms based on the criteria that the firms need to be among the largest in their respective subsectors. Firm size is measured using net assets. Appendix Table A3 provides list of sample firms in our final dataset where firms are ordered by size.¹⁰ The daily stock returns for each energy firm is the logarithmic difference of share price at time t and $t - 1$. Stock prices data is gathered from Thomson Reuters Datastream.

Table 1 provides subsector-wise stochastic properties of all firms in

our sample. The mean returns of the oil and gas (0.007%), multiline utilities (0.006%) and renewable energy (0.037%) subsectors are positive, while it is negative for the oil & gas related products and services (−0.025%) subsector. The standard deviation varies from 1.658% to 3.603% for the multiline utilities and the renewable energy subsectors, respectively, indicating that the renewable energy firms exhibit higher stock return volatility than that of the firms in the other three subsectors. The Sharpe ratio is negative for all four subsectors. The return series are negatively skewed, and they exhibit leptokurtic distribution (except the case of renewable energy subsector). The null hypothesis of normality, autocorrelation and homoscedasticity is respectively rejected by the Jarque-Bera test, the Ljung-Box test and the ARCH test.

4. Empirical analysis

We explain empirical results in four parts. In the first part, we present and describe results pertaining to conditional volatility and risk

¹⁰ We observe that oil and gas companies are relatively larger in size compared to other energy-related companies. This is potentially due to oil and gas company's involvement in all the segments of the business, such as exploration, production, refinement, transportation, marketing, and investment etc. The renewable energy companies appear to be the smallest in terms of size.

Table 2
Summary statistics of value-at-risk.

	Mean	Max	Min	Var	SD	Med	Skew	Kurt
Oil & Gas (OGC)	4.298	26.279	2.049	4.765	2.090	3.804	3.729	23.760
Oil & Gas Related Equipment and Services (OGES)	5.290	35.561	2.759	7.585	2.500	4.702	4.141	33.616
Multiline Utilities (MU)	3.570	18.321	2.206	2.010	1.379	3.203	4.171	29.341
Renewable Energy (RE)	7.996	28.579	3.832	7.927	2.597	7.498	1.840	8.718

Note. This table provides the average subsector-wise summary statistics of value-at-risk for the underlying firms. The value-at-risk is calculated by $q = 0.01$ and conditional volatility estimated by ARMA (1,1)-GJRGARCH (3, 3) framework with Gaussian distribution.

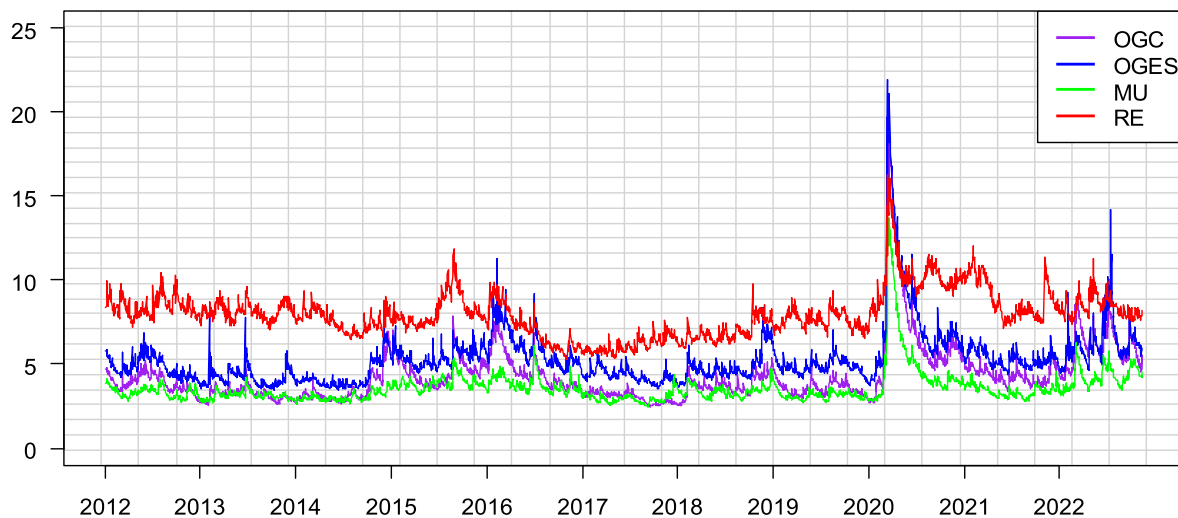


Fig. 2. VaR of each energy subsector.

Note. This figure reports the daily VaR with $q = 0.01$, averaged by energy subsectors. OGC: oil and gas; OGES: oil and gas related equipment and services; MU: multiline utilities, and RE: renewable energy. OGC, OGES, MU, and RE are respectively indicated by purple, blue, green, and red. VaR for each firm is calculated by the ARMA (1,1)-GJRGARCH (3,3) framework with Gaussian distribution. (For interpretation of the references to colour in this figure legend, the reader is referred to the web version of this article.)

exposure of the energy subsectors. In the second part, we analyze the common factor and investigate the correlation between common factor and several external market factors. The third part explains short- and long-term connectedness across firms derived from network topology and connectedness dynamics. The fourth part explains the nature of risk spillover among energy companies by presenting risk scores and decomposing them into firm-specific risk contributions.

4.1. Firm-specific conditional volatility and risk

To estimate daily conditional volatility, we select the best-fitted model, i.e., ARMA (1,1)-GJRGARCH (3,3) framework with Gaussian distribution. We standardize the conditional volatility series to zero-mean. The daily variance for individual firm is obtained and then averaged by group, shown in Fig. 1. A high homogeneity of volatility could be detected between the oil and gas and the oil and gas related equipment and services subsectors potentially due to their supply chain relationship.

Based on the univariate marginal distribution model, the estimation of VaR is conducted at the quantile level $q = 0.01$ for each company in our sample. For brevity, we present the summary statistics of the subsector VaR estimates in Table 2. It is found that, in terms of the mean VaR, the firms in the renewable energy subsector exhibit the highest concentration of tail risk (7.996%), and the firms in the multiline utilities subsector show the lowest amount of tail risk (3.570%). The mean VaR of firms in the oil and gas and oil and gas related equipment and services subsectors exhibit a tail risk of 4.298% and 5.290%, respectively. With regard to the volatility of the VaR estimates, the multiline utilities subsector exhibit the lowest standard deviation, while the

highest variation in VaR is observed for the renewable energy subsector.

Fig. 2 shows the time-varying development of VaR of the four underlying subsectors. In accordance with static VaR analysis, we aggregate firm-level VaR estimates and present subsector-wise dynamic VaR estimates. Like the static VaR estimates, lower and relatively stable VaR estimates are observed for the multiline utilities and oil and gas subsectors. The time varying VaR estimates of the renewable energy subsector are considerably higher than that of the other three underlying subsectors. During the oil crisis in April 2020, the oil and gas and oil and gas related equipment and services subsectors experienced extreme risk, due to the rapid crash of crude oil price. The subsectors, however, recovered quickly after the crude oil price rebounded. The abnormal VaR of the oil and gas related equipment and services subsector in July 2022 was primarily contributed by one company, Saipem (an Italian multinational oilfield services company and one of the largest in the world), whose new share issued was not fully subscribed by the market and was recognized as a company with long-term financial losses.¹¹

It is noteworthy that for the oil and gas, oil and gas related equipment and services, and multiline utilities subsectors, VaR increased at the end of 2014, reached a high value at the start of 2016 and reached another peak in December 2018. The 2014 increase in VaR estimates can be attributed to the significant deterioration in crude oil prices and a demand and supply imbalance while the high idiosyncratic risk of 2016 could be related to several global factors, such as high volatility in the

¹¹ Conditional volatility estimates of individual companies in the oil and gas related equipment and services subsector are available from the corresponding author on request.

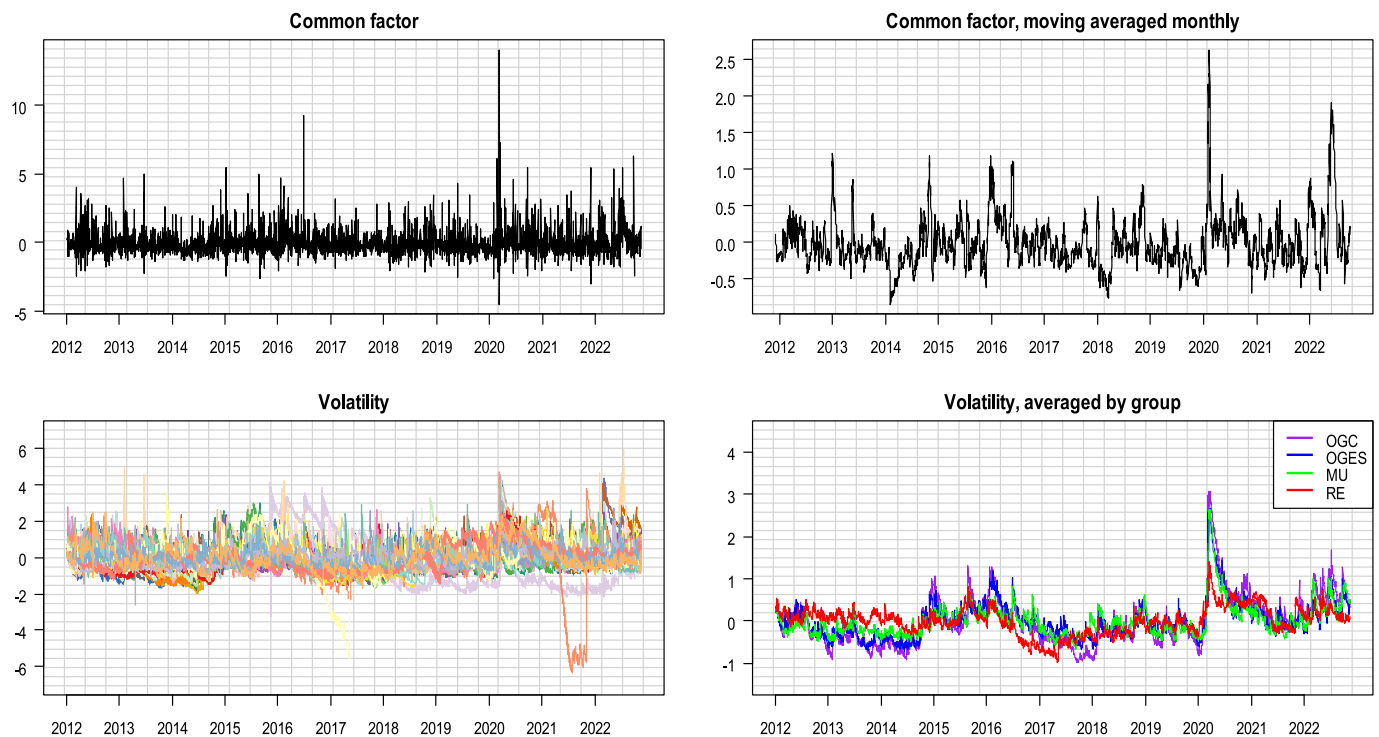


Fig. 3. Comparison of Common factor and volatility.

Note. We contemplate the full-period panel volatility of all firms as a 1st-order VAR-CF process. The sample length $T = 2835$. The top left figure shows the negative of common factor obtained from step 1–3 in section 2.2. The top right figure shows the negative of common factor with a smoothing period of a stock market month, i. e., 21 days. The bottom left figure shows the log conditional volatility after zero-mean standardization for each firm which is calculated by the ARMA (1,1)-GJR-GARCH (3,3) framework with Gaussian distribution. The bottom right figure shows the volatility averaged by each energy subsector. OGC: oil and gas; OGES: oil and gas related equipment and services; MU: multiline utilities, and RE: renewable energy. OGC, OGES, MU, and RE are respectively indicated by purple, blue, green, and red.

crude oil market, the Chinese stock market crash, a significant decline in the Dow Jones Industrial Average, low gas prices, and uncertainty surrounding the US Federal Reserve's move to raise interest rate (Chen et al., 2019). From mid-2016 onwards, the VaR declined to the pre-2014 level, which may be attributed to a relatively stable energy demand and supply from mid-2016 to 2018.

Compared to the other three subsectors, we observe a higher time-static risk exposure of the renewable energy subsector (Table 2) and the highest estimates of time-varying VaR with significant fluctuations over the sample span (Fig. 2). This higher uncertainty of the renewable energy subsector could be linked to specific risk factors associated with the renewable energy industry, such as technological innovation, uncertainty in the energy policy landscape, limited admittance to reserves for capital exhaustive renewable energy developments, and overall energy market risk (Alolo et al., 2020).

Further, we report the lowest tail risk exposure of the multiline utility companies both in the time-static and dynamic analysis. This finding may be linked to these companies' heterogeneous and diversified operations in utility generation, transmission, storage, processing, and retailing, etc. Moreover, the companies in this subsector are also mature and geographically well-diversified, making them more resilient towards geopolitical uncertainties.

Overall, in this subsection, we report that VaR estimates of the oil and gas and oil and gas related equipment subsectors increase significantly with the geopolitical uncertainty. This is intuitive as future investments and operations of firms in the oil and gas industry highly rely on an optimal and stable price of crude oil. Hence, uncertainties surrounding oil price directly influence firms' exploration and production activities in this subsector. The oil and gas related equipment and services companies, on the other hand, are indirectly impacted by geopolitical uncertainties as their business activities are highly cyclical and

rely on stable operations of the firms in the oil and gas subsector.

The results in this section also have economic implications. For instance, as we find higher tail risk exposure of the renewable energy companies in both time-static and time-varying analyses, portfolio managers holding investment in these companies should determine whether they have enough capital reserves to cover potential losses or high tail risk exposure would require them to reduce their investment concentration in these companies. Further, as we find that the oil and gas and the oil and gas related equipment subsectors' tail risk exposure increases with geopolitical uncertainty, relevant sectoral investors may need to develop appropriate strategies to hedge against geopolitical risks.

4.2. Common factor

To study the energy firms' risk network, multivariate time series of log conditional volatility after zero-mean standardization are considered as a VAR-CF process. To have enough degree of freedom, we consider the lag order $p = 1$ for vector autoregression and network estimation. The common factor appears as in Fig. 3. Many features are notable. Firstly, the common factor captures the risk inherent in the entire energy industry. The common factor during 2015–2016 has a higher value which is consistent with the higher volatility during the same period. The strike of common factor in 2020 is in line with the extreme event of oil price war.

Secondly, we find that the autocorrelation coefficient (derived from the Ljung-Box test) of the common factor is statistically significant (p -value < 0.01). Given that the common factor reflects systematic risk extracted from the volatility network, the autocorrelation of the common factor implies that the cross-sectional volatility clustering widely exists in the energy industry.

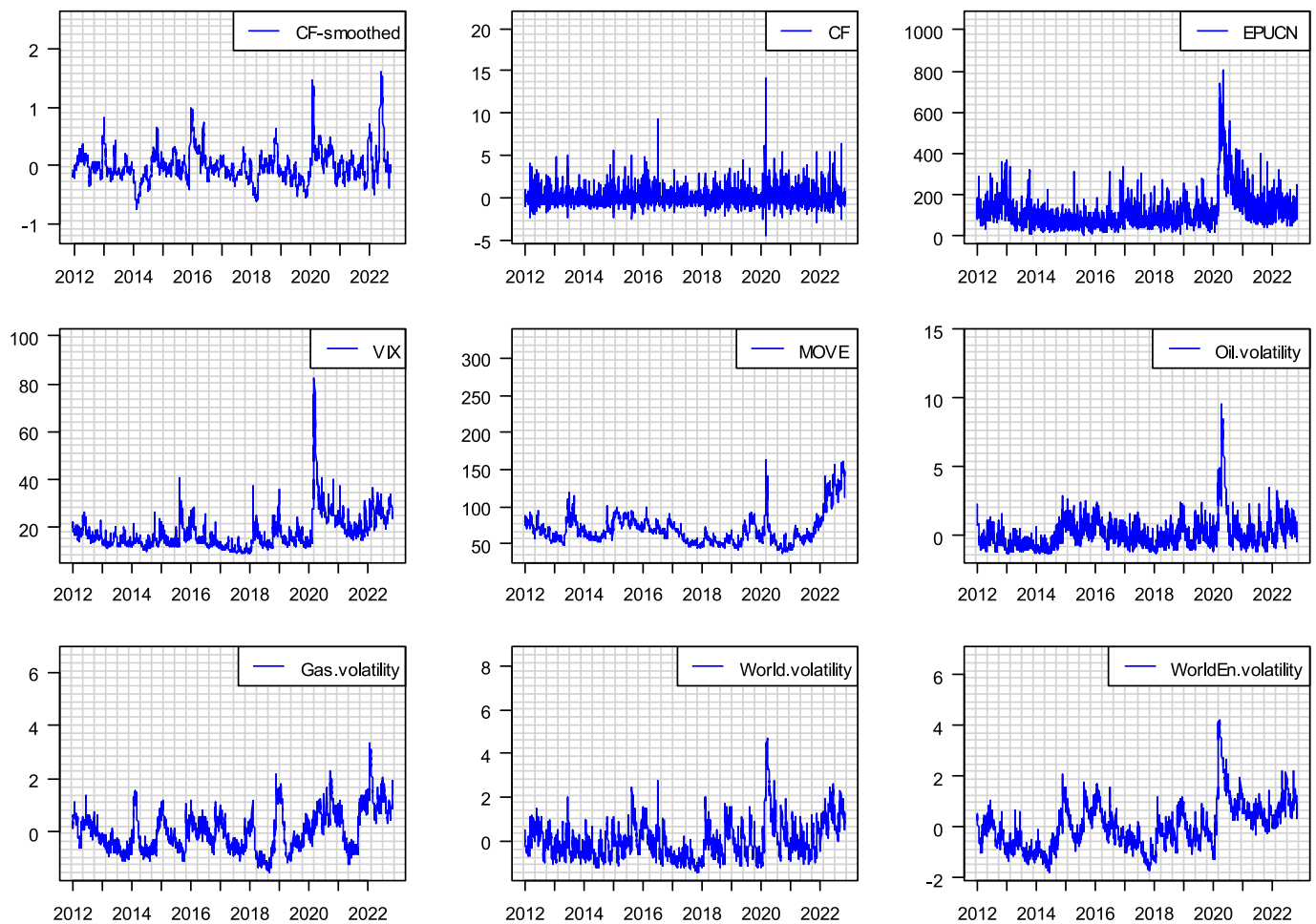


Fig. 4. Comparison of Common factor and market indices.

Note. The figure with legend CF-Smoothed shows the common factor with a smoothing period of a stock market month, i.e., 21 days. The legend CF denotes the common factor obtained from step 1–3 in section 2.2. We contemplate the full-period panel volatility of all firms as a 1st-order VAR process. EPUCN: US Economic Policy Uncertainty Index; VIX: CBOE Volatility Index; MOVE: implied bond volatility in the US Treasury market; Oil: the volatility of Crude Oil WTI Futures Price; Gas: the volatility of Natural Gas Futures Price; World: the volatility of MSCI World Index; World En: the volatility of MSCI World Energy Index. The volatilities are estimated with using the model explained in section 2.1, i.e., we use the log conditional volatility after zero-mean standardization for each firm that is calculated by the ARMA (1,1)-GJRGARCH (3,3) framework with Gaussian distribution.

Table 3

Correlation between common factor and market indices.

	CF	EPUCN	VIX	MOVE	Oil	Gas	World	World Energy
CF	1.000							
EPUCN	0.067	1.000						
VIX	0.168	0.589	1.000					
MOVE	0.126	−0.008	0.412	1.000				
Oil	0.238	0.452	0.550	0.264	1.000			
Gas	0.108	0.300	0.473	0.338	0.304	1.000		
MSCI World	0.208	0.395	0.813	0.477	0.534	0.386	1.000	
MSCI World Energy	0.212	0.494	0.794	0.340	0.694	0.462	0.761	1.000

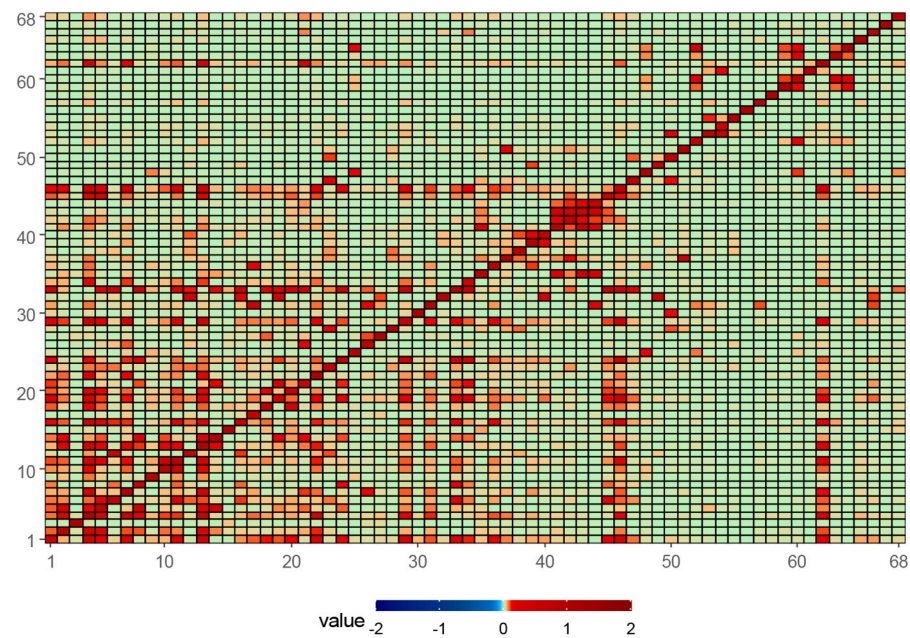
Note. The CF denotes the negative value of common factor, obtained from step 1–3 in section 2.2. We contemplate the full-period panel volatility of all firms as a 1st-order VAR process. EPUCN: US Economic Policy Uncertainty Index; VIX: CBOE Volatility Index; MOVE: implied bond volatility in the US Treasury market; Oil: the volatility of Crude Oil WTI Futures Price; Gas: the volatility of Natural Gas Futures Price; World: the volatility of MSCI World Index; World Energy: the volatility of MSCI World Energy Index. The volatilities are estimated using the model explained in section 2.1, i.e., we use the log conditional volatility after zero-mean standardization for each firm which is calculated by the ARMA (1,1)-GJRGARCH (3,3) framework with Gaussian distribution.

Thirdly, both the moving average of the common factor and the group average of volatility present a stronger trend and autocorrelation than that in the daily series. It means that market shocks impact energy firms in different time points with similar effect (increase/decrease risk). The common factor has long-term effects on firms, mathematically represented by the moving average process of long order from the VAR-

CF model. Thus, the common factor can capture not only an immediate shock, but also long-term effects in the energy market.

Afterwards, we investigate the components of the common factor. According to the literature, economic policy uncertainty, market risk, oil price shock are common risk factors for energy firms (Li et al., 2020; Natalia et al., 2018; Reboredo, 2015). Fig. 4 and Table 3 show the

Panel A: Connectedness obtained from VAR with common factors



Panel B: Connectedness obtained from VAR without common factors

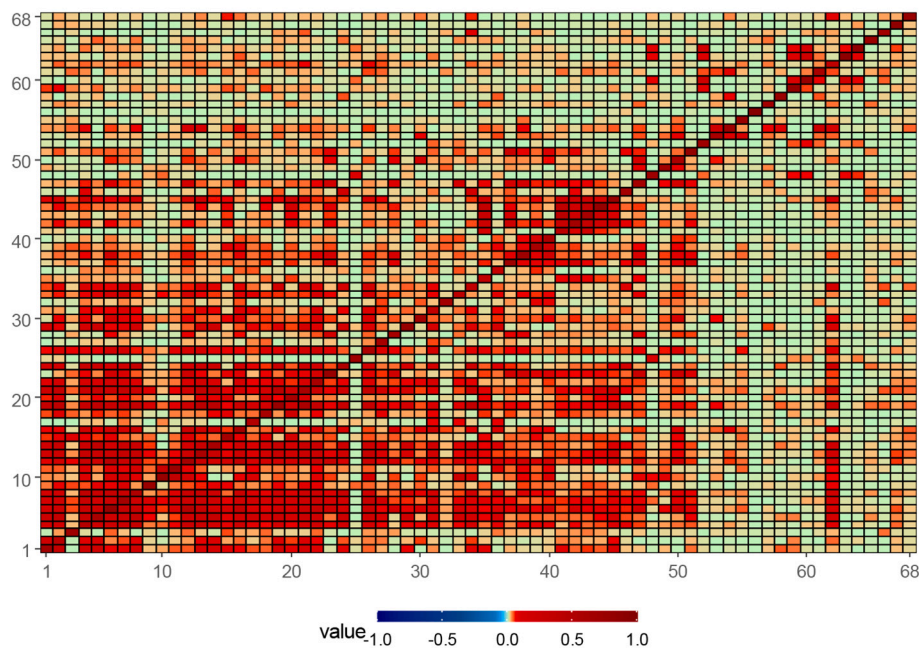


Fig. 5. Heatmap of connectedness.

Panel A: Connectedness obtained from VAR with common factors.

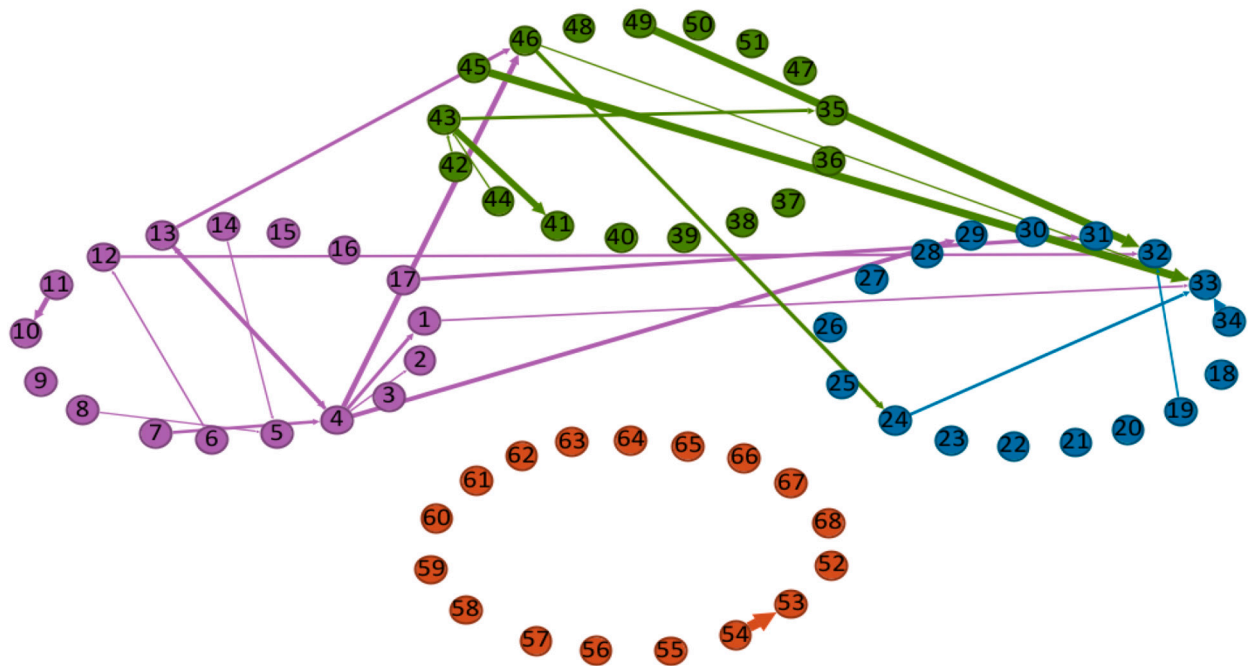
Panel B: Connectedness obtained from VAR without common factors.

Note. Panel A (Panel B) is obtained from high-dimensional VAR model with common factors (simple VAR model). We contemplate the full-period panel volatility of all firms as a 1st-order VAR process. The connectedness is obtained based on the extended DY (2014) framework in eq.(13), with $H = 10$, $P = 1$, $T = 2834$ trading days. The x-axis and y-axis respectively indicate source and target companies, whose names and numbers are shown in Appendix Table A3.

dynamics and correlation between the common factor and the US Economic Policy Uncertainty Index, CBOE Volatility Index (VIX), implied bond volatility in the US Treasury market (MOVE), volatility of Crude Oil WTI Futures Price, volatility of Natural Gas Futures Price, volatility of MSCI World Index, and volatility of MSCI World Energy Index. Interestingly, the common factor has a non-zero correlation with all the

external factors. The common factor's correlation with volatility of Crude Oil WTI Futures Price, volatility of MSCI World Index, and volatility of MSCI World Energy Index is stronger compared to the common factor's correlation with the VIX, MOVE, volatility of Natural Gas Futures Price and US Economic Policy Uncertainty (See Table 3). In addition, we implement multiple ordinary least squares regression of the

Panel A: Top 30 Connectedness



Panel B: Top 200 Connectedness

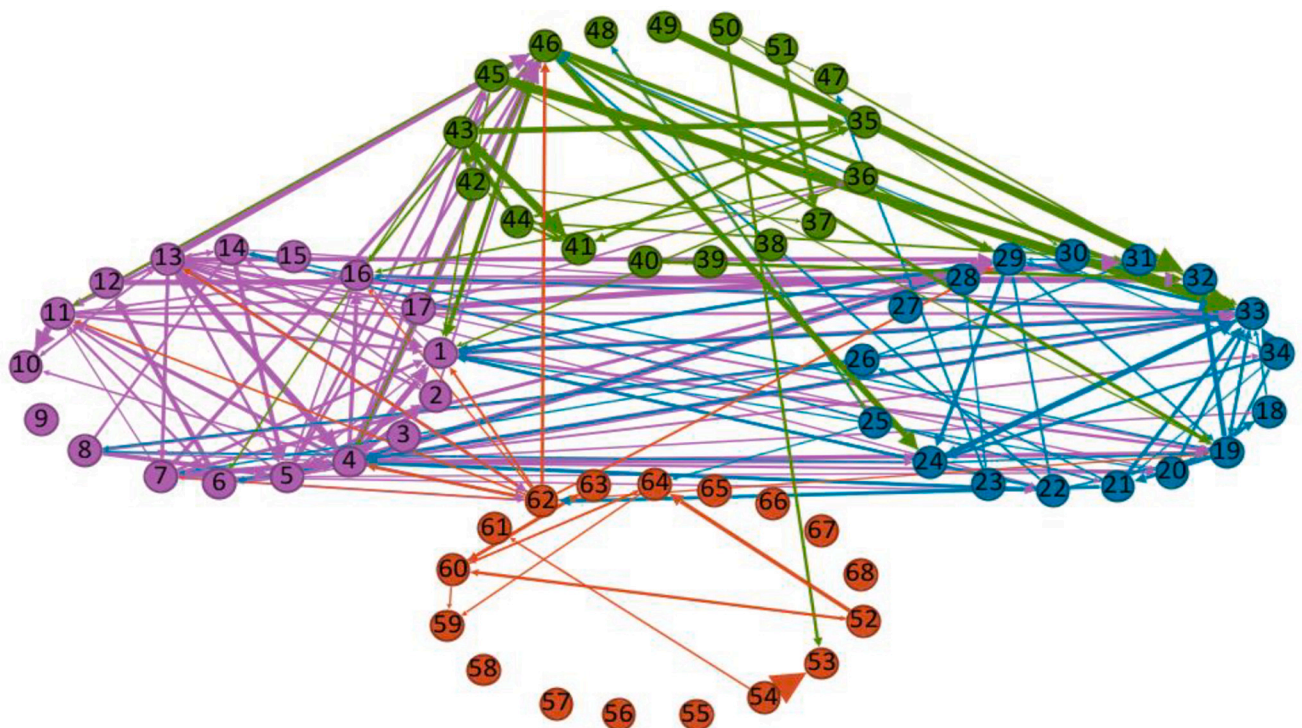


Fig. 6. Topological network of connectedness.

Panel A: Top 30 Connectedness.

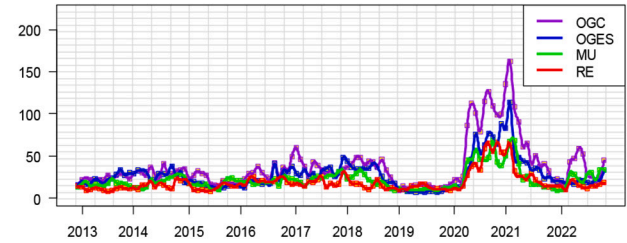
Panel B: Top 200 Connectedness.

Note. OGC: oil and gas; OGES: oil and gas related equipment and services; MU: multiline utilities, and RE: renewable energy. OGC, OGES, MU, and RE are respectively indicated by purple, blue, green, and red. The linkage in this figure is the adjacency matrix obtained from high-dimensional VAR model with common factors. We contemplate the full-period panel volatility of all firms as a 1st-order VAR-CF process, and then estimate the adjacency matrix of connectedness by the extended DY (2014) framework ($T = 2835$, $P = 1$, $H = 10$).

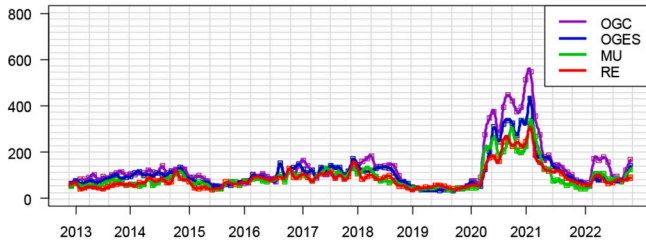
Panel A: Dynamics of connectedness



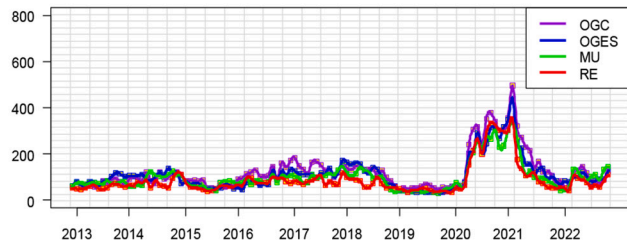
Panel B: Short-term connections inside each subsector



Panel C: Incoming connections for four industry subsectors



Panel D: Outgoing connections for four industry subsectors

**Fig. 7.** Aggregate and sector-wise connectedness.

Note. This figure reports the dynamics of connectedness over the energy market. The connectedness is estimated by VAR-CF model, estimated by rolling estimation with window size = 252, refit horizon = 21, $p = 1$, $H = 10$. The self-connections are not included. The y-axis marks the rolling window period that ends at that time point. OGC: oil and gas; OGES: oil and gas related equipment and services; MU: multiline utilities, and RE: renewable energy. OGC, OGES, MU, and RE are respectively indicated by purple, blue, green, and red. (For interpretation of the references to colour in this figure legend, the reader is referred to the web version of this article.)

common factor on all seven components and get an R-Squared value of 0.07116. This result indicates that the common factor cannot be fully explained by the investigated factors (See, Fig. 4). Within an autoregressive distributed lag (ARDL) model of Pesaran et al. (2001) with lag = 21, we get an R-Squared value of 0.6282.

4.3. Connectedness network analysis

We examine network connectedness between the firms in four underlying energy subsectors. The short-term and full sample period horizons are estimated respectively to analyze short- and long- term connectedness among energy firms. To have enough degree of freedom, we consider lag order $p = 1$ for vector autoregression and network estimation. In the full sample period horizon with $T = 2835$, the VAR is estimated following the same approach for consistent calculation and comparability. Following the DY (2014) framework, we apply generalized variance decomposition with $H = 10$, and generate the adjacency matrix. Fig. 5 shows the connectedness by a heatmap format. Figures in Panel A and Panel B are obtained respectively from high-dimensional VAR-CF and simple VAR models. The x- and y-axis respectively indicate source and target companies, whose names and numbers are shown in Appendix Table A3. Panel A shows a lighter colour than Panel B as the setting of common factor in VAR removes cross-sectional dependence among firms caused by homogeneous effects of external factors.

Fig. 6 represents elliptical and topologicals network of the full sample period horizon. A linkage in this topology indicates an entry of θ_{ij}^H in eq. (13), i.e., a shock of a production firm enhances volatility of a target firm. The firms in our sample are denoted as 1, 2, 3..., 68 and are presented in the nodes. To capture strong connectedness among energy firms, Panels A and B show top 30 and top 200 linkages respectively. The self-connections are not shown in this figure.

In general, connectedness between companies in the same subsector is stronger than that between firms from different subsectors. The oil and gas companies have the strongest connectedness within the same

subsector which could be linked to overlap of costs and benefits, subsector industrial energy demand, and endogenous substitution effect (see, Agnolucci et al., 2017; Chakravorty et al., 1997). Relatively weaker linkage between firms from other subsectors could be attributed to global climate change effects and oil price shocks (Madlener and Stagl, 2005; Pham, 2019).

The multiline utilities subsector exhibits a high number of connections with other underlying subsectors. For example, MDU Resources Group, Centrica, and EVN (numbered 45, 46, 49 respectively), among others, from the multiline utilities subsector appear to have high connections with oil and gas related equipment and services companies, Saipem, National Oilwell Varco, and Amec Foster Wheeler (numbered 33, 24, 32 respectively). This is per the public policy landscape about energy products and services that could affect both the subsectors.

We also observe connectedness in the companies' supply chain. For instance, Royal Dutch Shell (numbered 4) has strong impact on Centrica (numbered 46) possibly because Royal Dutch Shell is an oil and gas exploration company while Centrica's principal activity is the supply of gas and electricity. Further, Centrica's strong connections with National Oilwell Varco and Amec Foster Wheeler (as mentioned in the previous paragraph) may be attributed to the fact that the latter two companies provide equipment, technologies, expertise and consultancy to their upstream oil and gas companies (potentially Centrica is one of them). The evidence of connectedness in the companies' supply chain has economic implications. For example, heightened distress in one company may propagate through interconnections between firms in the upstream and downstream in the supply chain increasing contagion risk and reducing potential diversification benefits.

We also observe strong connections within the oil and gas (numbered 1 to 17) and oil and gas related equipment and services subsectors (numbered 18 to 34). This may arise as these two industries are susceptible to crude oil and gas price changes and geopolitical uncertainties, while multiline utility firms are more robust to oil price uncertainty due to their diversified nature of operations. Relatively

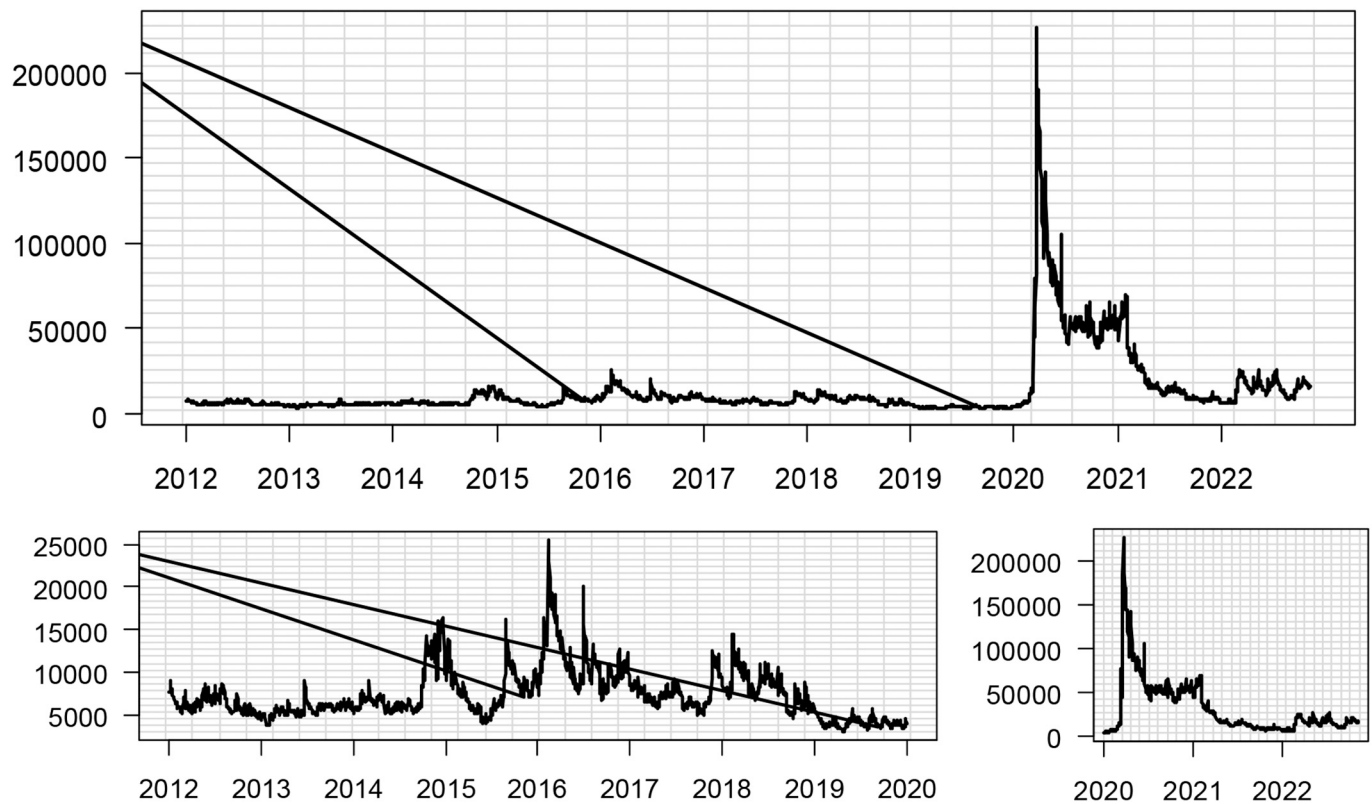


Fig. 8. Systemic risk score.

Note. The top figure shows the systemic risk score, obtained follows eq.(14). The rolling panel adjacency matrices are obtained with window size = 252, refit horizon = 21, $p = 1$, $H = 10$. The daily VaR in $q = 0.01$ is utilized as composition level. For a clearer visualization, the results before and after 2020 are plotted separately in the bottom panels.

higher amount of bidirectional connectedness exists between the firms in the oil and gas and oil and gas related equipment and services subsectors. It can be noticed that there are more outgoing connections from the oil and gas and to the target oil and gas related equipment and services subsector.

In the case of firms in the renewable energy subsector (firms numbered from 52 to 68), we observe fewer connections within the same and other subsectors. This strong heterogeneity may primarily be attributed to distinguished responses to oil price, various policy impacts, and regional disparity, as proved by Pham (2019), Steffen (2020), Abrell et al. (2019), Alolo et al. (2020). Green Plain (numbered 62) is the only renewable energy company that has strong connectedness with the oil and gas and oil and gas related equipment and services subsectors which could be attributed to the fact that Green Plain transforms crops into specialty alcohols and low-carbon fuel. Different from wind and solar energy, fuel prices such as oil and gas prices are highly correlated to each other which breeds the connectedness. Uniquely, Pennon Group (numbered 50) in the multiline subsector has strong connectedness with Vestas (numbered 53) in the renewable energy subsector. This finding may arise as both companies have proposed strong environmental, social and governance (ESG) concepts, received sustainable offer, and gained investor confidence in recent years.

It is noteworthy that Figs. 5 and 6 present the adjacency matrix and network plot respectively for the entire sample period. Although this analysis provides an overview of long-term interconnectedness, it has been widely acknowledged that the relationship among asset prices may exhibit a time-varying behavior (Bekiros et al., 2017; Mensi et al., 2017). To this end, we estimate network connectedness in the short-term setting. This exercise examines potential dynamic shift in the connectedness structure which has implications for portfolio uncertainty diversification and downward uncertainty optimization.

For the short-term horizon, we estimate the VAR-CF model with rolling window size = 252, refit horizon = 21, $p = 1$, $H = 10$. Fig. 7 presents short-term aggregate and subsector-wise connectedness. Note that y-axis marks the rolling window period that ends at that time point. For instance, the value marked on January 1, 2013 denotes the connectedness estimated during the period ranging from January 1, 2012–December 31, 2013.

We observe three cycles of connectedness in 2012–2015, 2016–2019, and 2020–2021, with the peak value of connectedness in each cycle is 469.1099, 684.8455, and 1623.296 respectively. They correspond to the oil price crash in 2014 (as shown in Appendix Fig. A6), the worldwide bull stock market in 2017 (as shown in Appendix Fig. A1 – A5), and the COVID-19 crisis in 2020. Note that the highest connectedness is not observed during the burst time of COVID-19. Instead, the COVID-19 crisis caused a long-term effect where the connectedness continuously intensified until the first quarter of 2021. This could be related to the quarantine policy, economic stagnation, and pessimistic market expectations. In 2022, we notice a new round of connectedness which may be linked to the Russia-Ukraine war and global energy shortage. Interestingly, in the full sample period panel ($T = 2087$), the sum of connectedness among all energy firms is 134.5874. We, therefore, notice higher connections in the short-term horizon indicating that short-term connectedness partially dissipates in the long-term.

Fig. 7B shows the dynamics of the connections within each subsector, named as internal connectedness. We find that the highest internal connectedness exists in the oil and gas subsector, especially after the burst of COVID-19. During 2015–2016, we find an increase in the number of connections in the multiline utilities subsector. This result, firstly, can be attributed to the period of financial and economic prosperity, and secondly, is in accordance with the previous literature (Dutta, 2018; Liu et al., 2017). The renewable energy subsector,

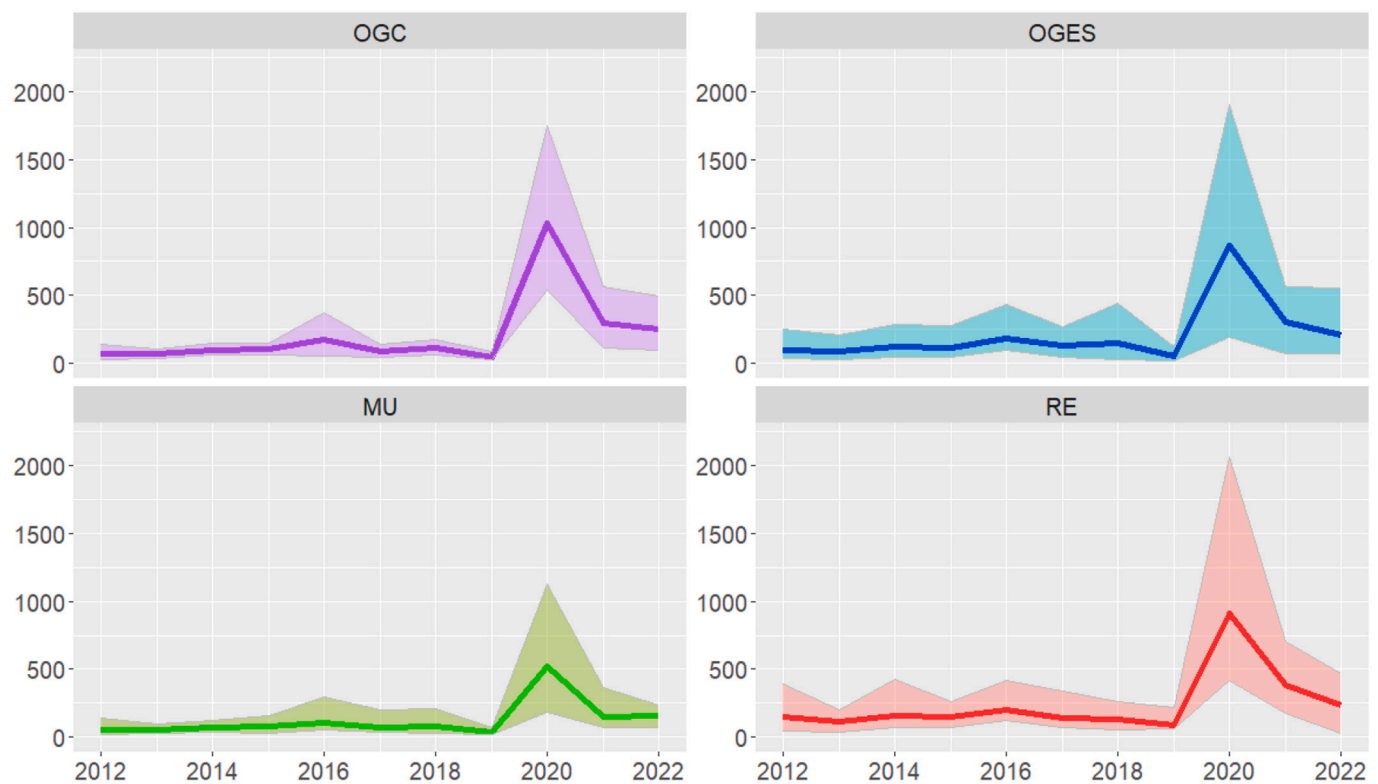


Fig. 9. Dynamic ranges of systemic risk contributions of each energy subsector.

Note. For each figure that represents one subsector, the firms with highest risk contribution is plotted as the top line, while the smallest contribution is plotted as the lower limit. The aggregated risk is decomposed by eq. (15–16), where the aggregated risk is induced from short-term adjacency matrix and daily VaR in $q = 0.01$ as composition level. OGC: oil and gas; OGES: oil and gas related equipment and services; MU: multiline utilities, and RE: renewable energy. OGC, OGES, MU, and RE are respectively indicated by purple, blue, green, and red. (For interpretation of the references to colour in this figure legend, the reader is referred to the web version of this article.)

however, exhibits a significantly low number of connections in 2015.

Fig. 7C and D report the sum of incoming and outgoing connections in the short-term horizon. For the oil and gas subsector in Fig. 7C, significant asymmetric variations are observed in the connectedness across time. Compared with others, the firms in the renewable energy subsector exhibit a lower number of outgoing connections to the firms in the other subsectors before 2020. During 2020–2021, the outgoing connectedness of the renewable energy firms increased substantially indicating that the impact of the renewable energy subsector increases during a crisis time. The net value of connectedness (incoming minus outgoing) in 2020–2021 reveals that the oil and gas subsector is a receiver of spillover risk while renewable energy firms serve as transmitter. The impact of the renewable energy subsector could be attributed to the long-term influence of renewable energy utilization on economic growth (Dogan et al., 2020) and an increased concern surrounding environmental sustainability issues (Nations, 2018). These factors are eventually resulting in a gradual shift from conventional towards clean energy sources. During 2016–2019, we observe a cycle of growth and decline in the level of connectedness. Interestingly, after periods of market adjustment, the idiosyncratic connectedness of the energy market tends to return to a low level. Although we find no evidence that the total value of connectedness in the energy market has a continuous upward trend, the outgoing spillover role of the oil and gas subsector is slowly transposed to the renewable energy subsector.

To summarize network connectedness results (derived from static and dynamic analysis) in this subsection, we observe strong (weak) connectedness within (across) the subsector(s). We further find that (i) the oil and gas companies have the strongest connectedness within the same subsector (Fig. 6), (ii) the multiline utilities subsector exhibits a high number of connections with other underlying subsectors, (iii) there

is strong bidirectional connectedness between oil and gas and oil and gas related equipment and services firms, and (iv) the renewable energy subsector has fewer connections within and across the subsectors. Additionally, in the dynamic connected analysis, we find that the oil and gas subsector shows high internal connectedness after the COVID-19 crisis while outgoing connectedness of the renewable energy firms increased in 2020–2021 indicating the renewable energy subsector's higher impact during a crisis. These results also have economic implications. For instance, since the renewable energy subsector has the weakest connectedness across the subsectors, a portfolio combining investment in the renewable energy and other energy related subsectors may provide highest diversification benefits. On the other hand, oil and gas and oil and gas related equipment and services firms will increase contagion risk due to their strong bidirectional connectedness.

4.4. Systemic and spillover risk

Given the connectedness across energy firms presented in the previous subsection, firm-specific risk should not be regulated separately without accounting for potential spillover risks from other firms. It is both a firm's idiosyncratic risk (source) and its connectedness with other firms (channel) that determine possible failure of a whole industry. Therefore, we quantify the systemic risk in a network by combining the adjacency matrix with the compromise loading of the risk level. We calculate the systemic risk and decompose the risk contribution of each firm in our sample. In addition, we decompose the risk score into the sum of the spillover effects of each pair of companies. Overall, this analysis enables us to identify systemically important firms that can assist policymakers and regulators in devising a roadmap to decouple the impact of risk spillover from one asset or sector to other assets or

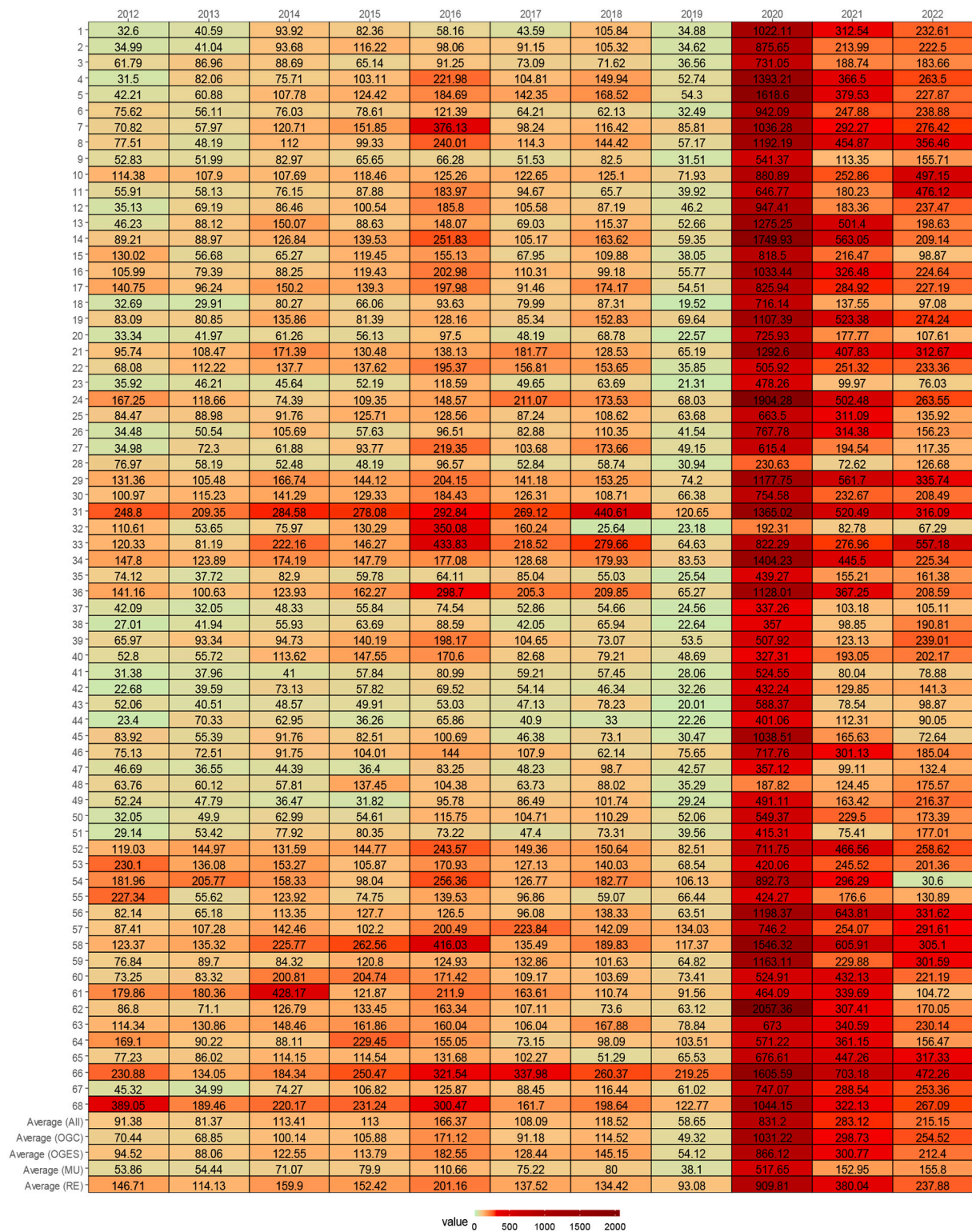


Fig. 10. The range of risk contribution of four energy subsectors.

Note. The systemic risk contributions are induced from short-term adjacency matrix and the daily VaR in $q = 0.01$ as composition level, based on eq. (16).

sectors.

Fig. 8 presents the dynamic development of the systemic risk score, reflecting the aggregated risk of all firms in the energy market. In general, we observe a significant fluctuation in the systemic risk score over time. Between 2012 and 2014, the systemic risk remained relatively low and stable. However, it increased gradually at the beginning of 2014 to mid-2014 and then reverted to the pre-2014 level. Interestingly, the risk

score increased dramatically since the end of 2014 and remained significantly high throughout 2015. The systemic risk score is substantially higher in 2016 compared to that in previous years. At the beginning of 2020, the systemic risk score jumped dramatically, while its fall back took almost two years. Overall, the simultaneous occurrence of the extreme idiosyncratic risk and high connectedness caused market-wide spillover.

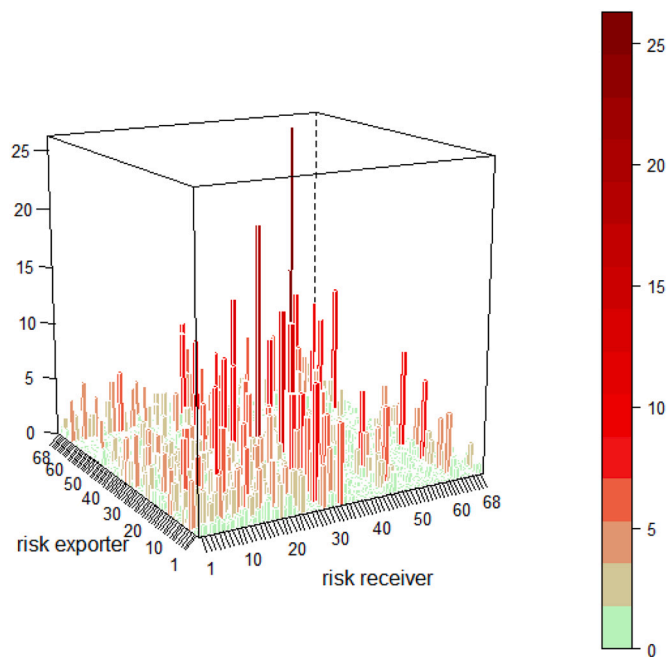


Fig. 11. Spillover risks in 3-Dimensional bar chart form.

Note. The calculation of risk spillover follows eq. (17) which combines risk level of source and target companies, and the connection that indicates the interaction of risks. The taller bar indicates that the risk spillover is stronger. The on-diagonal entries of spillover are zero due to the zero value of diagonal entries in the adjacency matrix.

Fig. 9 plots the dynamic ranges of systemic risk contributions for each subsector. The firms in the subsector with the highest risk contribution is plotted as the topper line, while the smallest contribution is plotted as the lower limit. It can be noticed that the trend for the four groups is broadly consistent, with high points occurred in 2016 and 2020. One may attribute this as the homogeneity in both idiosyncratic risk and connectedness that we find in previous subsections. Our findings of increased risk contribution in 2016 is a consequence of high idiosyncratic risk not the connectedness accumulation, while the high-risk contribution in 2020 is the joint results from both high idiosyncratic risk and high connectedness in accordance with our previous analyses.

The special character of the renewable energy subsector is obvious. The features of the renewable energy subsector during 2012–2019 are distinguished clearly by high systemic risk importance, extremely high value of idiosyncratic risk, and low connectedness. During 2020–2021, high connectedness and idiosyncratic risk of the renewable energy sector implies that the sector has been the largest systemic risk contributor. However, this phenomenon is inferred to be temporary, because there are still a limited number of network linkages between the renewable energy and the other subsectors. This finding is consistent with our previous results. For instance, in Fig. 6, we reported that among the four subsectors, the risk contributions are typically higher for the renewable energy subsector. As shown in Table 2, the VaR of the renewable energy subsector is much larger than that of the multiline utilities subsector. Additionally, in Fig. 7B, the overall systemic contribution of the multiline utilities subsector was reported to be relatively lower than that of renewable energy subsector, while the connectedness of the multiline utilities subsector was far more than that of the renewable energy subsector.

Although the renewable energy subsector has gained more attention because of global warming and climate change issues and experienced significant investment growth, the subsector is still in the developing phase. It disproportionately relies on technological innovation, funding, and policy support. Concerning systemic risk regulation, it is important

to control the idiosyncratic risk by improving the stability of technological innovation, budget, and policy supports instead of cutting the risk channel between the renewable energy and the other subsectors.

Fig. 10 reports systemic risk contributions of individual companies on an annual basis. We utilize the short-term adjacency matrices to approximate the risk contributions for the dynamic horizon. We observe that a company's systemic importance changes over time. For example, Vallourec (numbered 31) appears to be a significant contributor to systemic risk in 2012–2018; however, it turns out to be an insignificant contributor in 2019. Further, Green Plains (numbered 62) made a major contribution to systemic risk in 2020, however, it made an average contribution in other years.

We now examine the intergroup risk spillover both in time-static and time-varying settings. Fig. 11 presents the spillover risk in a 3-Dimensional bar chart form. The diagonal entries denote the self-contribution of risk spillover. The off-diagonal entries denote the risk spillover that considers the connection between two companies and the risk level of each company.

It is indicative that a high value of spillover risk always occurs between firms with similar sizes and within the same subsector. The entries close to the diagonal have a higher value of spillover risk. As we number the firms in each subsector by ranking the market value of firms, the entries closed to the diagonal always have similar sizes and belong to the same subsector. It is also in line with the previous literature that reports positive correlations among size, competition, similarity, and spillover effects (Gong, 2018). In addition, in the renewable energy subsector, we find that within-sector variations contribute significantly to the overall risk. This result is also consistent with our previous findings.

We now examine the dynamic spillover among different subsectors in Fig. 12. Similar to the static spillover, the diagonal plots indicate the within-subsector risk spillover variations. During the COVID-19 pandemic and the oil price war in 2020, the oil and gas related equipment and services and multiline utilities subsectors received approximately similar risk contribution from the oil and gas subsector. However, the renewable energy subsector received lower risk spillover than other subsectors from the oil and gas subsector. From 2020 to 2021, unlike other group pairs, the spillover risk inside the renewable energy subsector increased substantially due to high level of idiosyncratic risk.

5. Conclusion

While systemic risk is well-investigated in the financial sector, the nature and extent of risk dependence or spillover across energy companies are still under-researched. This paper adds to the literature in three aspects. First, the previous studies mostly ignore heterogeneity in firm-level risk spillover and concentrate on only the oil and gas subsector. We, therefore, contribute by exploring risk spillover at the firm level, considering a large sample of 68 companies in four energy-related subsectors. Second, we use a novel approach to estimate connectedness. The high-dimensional network among energy companies is constructed based on a VAR-CF model and an extended DY (2014) framework. Third, we propose novel modelling of systemic risk that comprise the network connectedness with the firm-specific idiosyncratic risk. This exercise enables us to complement the full picture of systemic risk that depicts the network's nodal driver and topological dynamics.

We report cyclical intensification of systemic risk in energy industry which is attributed to heterogeneous factors, such as oil price crash, bull stock market globally, the COVID-19 crisis, and the Russia-Ukrainian War. Regarding the time horizons, the short-term network has higher connectedness than the long-term, i.e., most connectedness disappears after a certain period with a special event. Among the four groups, the renewable energy subsector ranks first in the systemic risk contributions. Before 2020, the high contribution of the renewable energy sector is mainly driven by high idiosyncratic risk not the intergroup connectedness, while after 2020, the spillover impact of the renewable energy sector becomes more powerful. We also find that the long-term

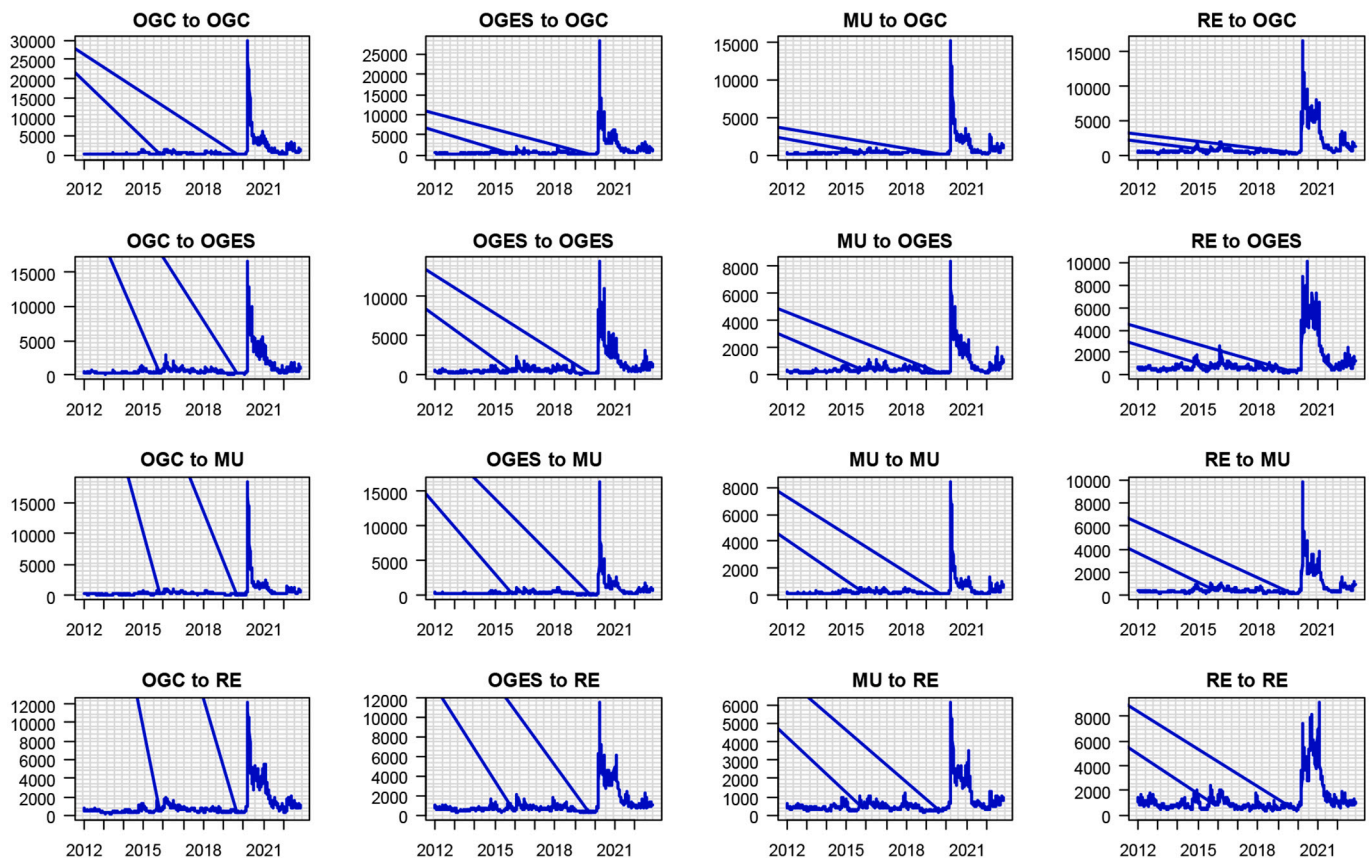


Fig. 12. The intergroup spillover risks.

Note. The intergroup spillover risks are obtained based on eq. (18), where daily VaR is used as comprise loading, and the adjacency matrices are induced by short-term panel. OGC: oil and gas; OGES: oil and gas related equipment and services; MU: multiline utilities, and RE: renewable energy. OGC, OGES, MU, and RE are respectively indicated by purple, blue, green, and red. (For interpretation of the references to colour in this figure legend, the reader is referred to the web version of this article.)

relationship between oil and gas and oil and gas related equipment and services firms are very significant. Finally, significant spillover risks are more often to occur between two firms with similar firm size and sub-sector, which could be related to the sector-wide homogeneity and competition.

Our results can assist risk managers of energy companies in (i) understanding high dimensional dynamics of the global energy companies and (ii) developing strategies to mitigate risk arising from other energy-related companies. Further, our findings can provide important inputs to international portfolio managers in devising asset allocation and hedging strategies concerning global energy-related companies.

This paper also opens several avenues for future research. For instance, we have relied on GARCH models for volatility estimation. It would be interesting to see whether results pertaining to risk transmission in the energy sector are sensitive to other types of volatility models such as multivariate stochastic volatility model. Further, while we mostly estimate uncertainty connectedness and spillover among the top energy companies, the empirical use of the connectedness measure for portfolio construction and/or derivation of warning signs for

policymakers would novel agenda for future research.

CRediT authorship contribution statement

Gazi Salah Uddin: Conceptualization, Writing – original draft, Writing – review & editing, Supervision. **Tianqi Luo:** Data curation, Software, Methodology, Writing – original draft, Methodology, Software, Data curation. **Muhammad Yahya:** Writing – original draft, Writing – review & editing, Supervision, Data curation, Validation. **Ranadeva Jayasekera:** Supervision, Investigation, Writing – review & editing. **Md Lutfur Rahman:** Writing – original draft, Validation, Writing – review & editing. **Yarema Okhrin:** Writing – review & editing, Formal analysis, Methodology, Software.

Acknowledgement

This paper was funded by the National Science Centre, Poland (Grant no. UMO-2014/13/B/HS4/01556).

Appendix A. Appendix

Table A1

Correlation coefficients.

Probability	BP	Chevron	ConocoPhillips	Exxon Mobil	Royal Dutch Shell	DataStream World Energy	DataStream World
BP	1.000						
Chevron	0.649 (15.335***)	1.000					
ConocoPhillips	0.570 (12.496***)	0.751 (20.494***)	1.000				
Exxon Mobil	0.580 (12.803***)	0.770 (21.741***)	0.643 (15.102***)	1.000			
Royal Dutch Shell	0.696 (17.444***)	0.672 (16.321***)	0.594 (13.304***)	0.617 (14.105***)	1.000		
DataStream World Energy	0.694 (17.329***)	0.794 (23.539***)	0.775 (22.101***)	0.732 (19.324***)	0.706 (17.946***)	1.000	
DataStream World	0.496 (10.277***)	0.556 (12.029***)	0.559 (12.130***)	0.517 (10.861***)	0.518 (10.903***)	0.789 (23.094***)	1.000

Notes: This table presents bivariate correlation coefficients of stock returns of large energy companies, aggregate energy sector, and aggregate stock market. *** indicates statistical significance at the 1% level.

Table A2

British Petroleum's top ten relationships.

Relation Type	Rank	Company	Overlapping relationship				
			Royal Dutch Shell B	Exxon Mobil	Chevron	Total	Eni
Supplier,Customer,Partner	1	Ithaca Energy	✓	✓			
Supplier,Partner	2	TechnipFMC Rg	✓	✓	✓	✓	✓
Supplier,Partner	3	Aker BP				✓	✓
Supplier,Partner	4	Noble Energy	✓				
Supplier,Partner	5	Linde	✓	✓	✓	✓	
Supplier,Partner	6	Empresas Copec		✓			
Supplier,Customer,Partner	7	BP Midstream Partners	✓	✓	✓		
Supplier,Partner	8	New Zealand Refining		✓			
Supplier,Customer,Partner	9	Gevo	✓			✓	
Supplier	10	Odfjell Drilling				✓	

Source: FactSet

Table A3

List of firms in the sample.

No.	Name	Market Value (USD)	Sub-sector	No.	Name	Market Value (USD)	Sub-sector
1	ExxonMobil	469,246.10	OGC	35	Sempra Energy	48,611.61	MU
2	Chevron Corporation	360,546.30	OGC	36	Électricité de France	47,941.70	MU
3	Reliance Industries	213,981.21	OGC	37	National Grid	42,986.09	MU
4	Royal Dutch Shell	196,939.63	OGC	38	Engie	35,182.56	MU
5	ConocoPhillips	166,923.60	OGC	39	RWE	27,778.75	MU
6	Total	154,248.26	OGC	40	E.ON SE	23,833.78	MU
7	Statoil	112,317.63	OGC	41	Ameren	21,540.06	MU
8	BP	102,970.95	OGC	42	PPL	20,182.48	MU
9	Saudi Basic Industries Corporation	67,483.25	OGC	43	CMS Energy	16,956.50	MU
10	Gazprom	66,273.79	OGC	44	NiSource	10,482.32	MU
11	Lukoil	53,328.05	OGC	45	MDU Resources Group	6149.32	MU
12	Eni	52,659.46	OGC	46	Centrica	5726.09	MU
13	Suncor Energy	49,596.69	OGC	47	Hera	4013.15	MU
14	Hess Corporation	44,883.52	OGC	48	Shenergy	3776.36	MU
15	PTT Public Company Limited	27,644.16	OGC	49	EVN	3302.71	MU
16	Repsol	20,637.81	OGC	50	Acea SpA	2927.16	MU
17	Inpex Corporation	15,645.05	OGC	51	Pennon Group	2872.14	MU
18	Enbridge Inc.	84,669.78	OGES	52	Sungrow	25,795.75	RE
19	Schlumberger	77,734.75	OGES	53	Vestas	25,611.90	RE
20	TC Energy	48,261.38	OGES	54	First Solar	16,035.62	RE
21	Halliburton Company	35,177.73	OGES	55	Siemens Gamesa Renewable Energy	12,671.63	RE
22	Tenaris	19,499.51	OGES	56	GCL-Poly Energy Holdings	8302.26	RE
23	Snam	16,197.49	OGES	57	VERBIO Vereinigte BioEnergie	5525.57	RE
24	National Oilwell Varco	9258.41	OGES	58	SunPower Corp	3891.24	RE
25	China Oilfield Services Ltd.	7290.33	OGES	59	Xiangtan Electric Manufacturing	3474.01	RE
26	Aker Solutions	5736.43	OGES	60	Risen Energy	3426.07	RE
27	WorleyParsons	5262.32	OGES	61	Canadian Solar	2325.25	RE
28	Enagás	4557.38	OGES	62	Green Plains	2166.06	RE
29	Scorpio Tankers Inc.	2750.56	OGES	63	Jiangsu Akcome Science & Technology	1995.93	RE
30	SBM Offshore	2724.90	OGES	64	Shanghai Aerospace Automobile Electromechanical	1957.48	RE

(continued on next page)

Table A3 (continued)

No.	Name	Market Value (USD)	Sub-sector	No.	Name	Market Value (USD)	Sub-sector
31	Vallourec	2718.67	OGES	65	CropEnergies	1392.95	RE
32	Amec Foster Wheeler	2527.34	OGES	66	Suzlon Energy	1296.12	RE
33	Saipem	2126.69	OGES	67	Motech Industries	310.35	RE
34	Wood Group	1295.50	OGES	68	Pacific Ethanol	276.60	RE

Note. Top firms in each subsector are selected based on market capitalization. OGC: oil and gas; OGES: oil and gas related equipment and services; MU: multiline utilities, and RE: renewable energy.

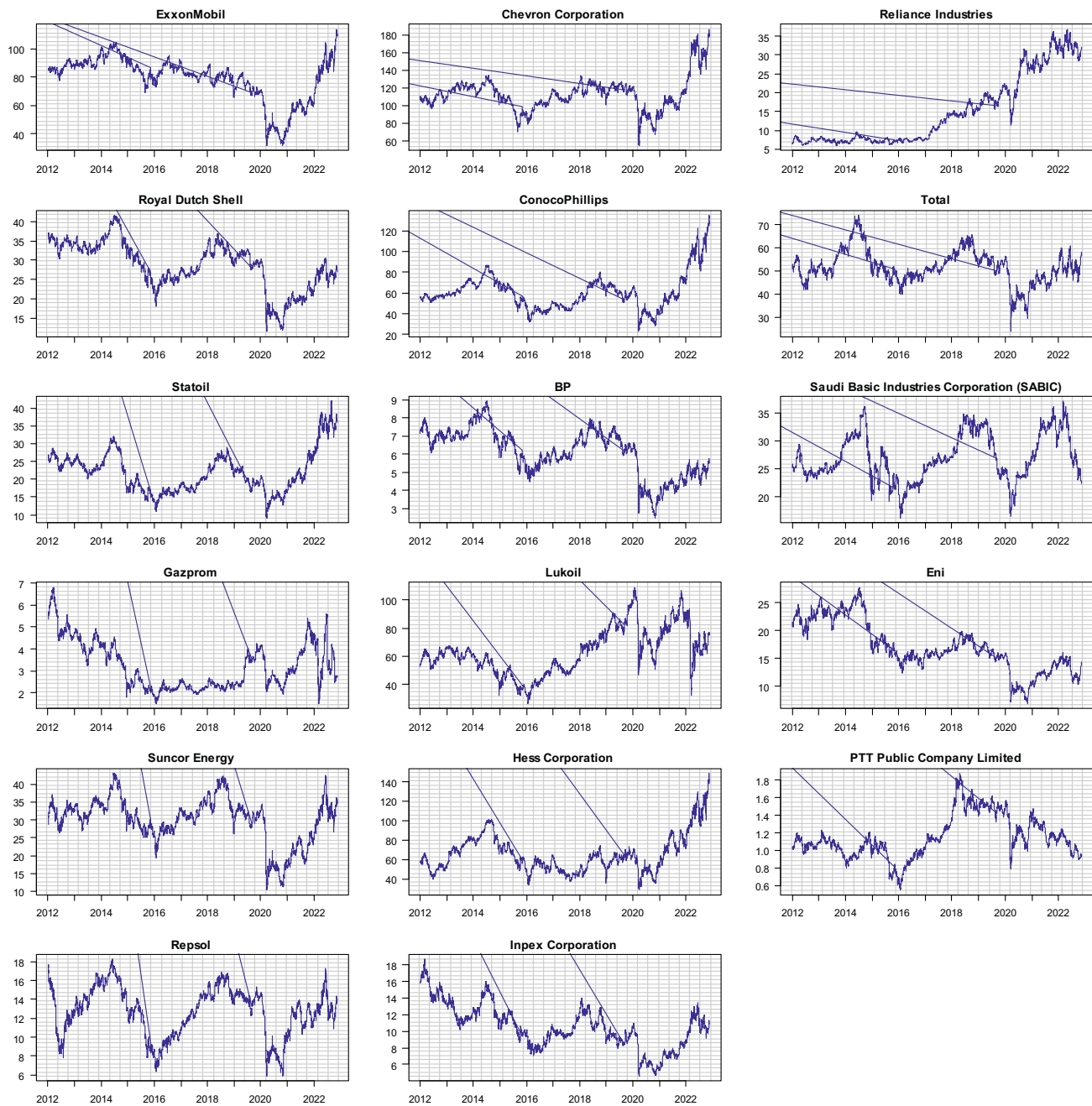


Fig. A1. Daily stock price trend of firms in the oil and gas subsector

Note. The daily stock prices of companies in the oil and gas subsector are shown in this figure.

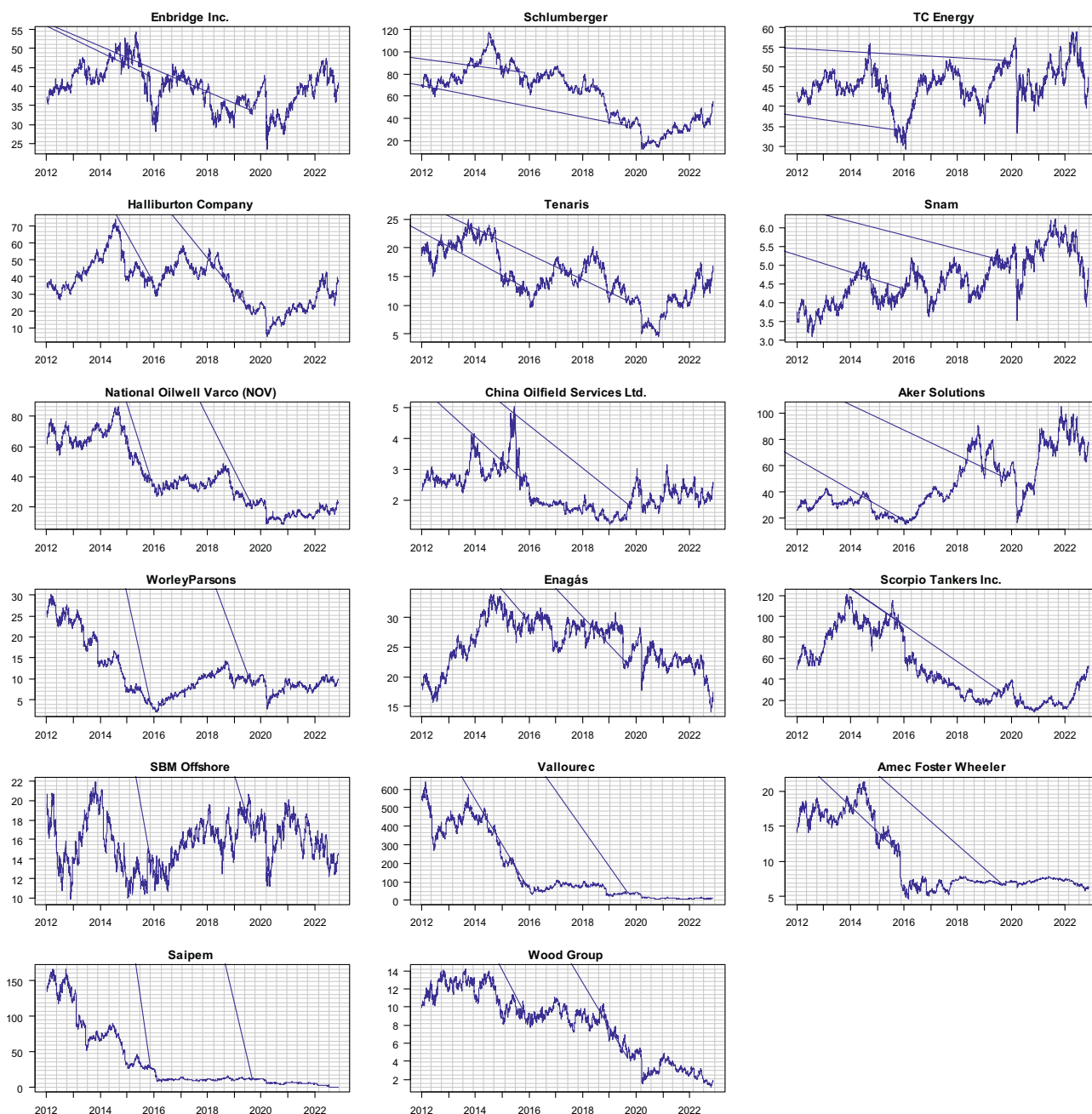


Fig. A2. Daily stock price trend of firms in the oil and gas related equipment and services subsector.

Note. The daily stock prices of companies in the oil and gas related equipment and services subsector are shown in this figure.

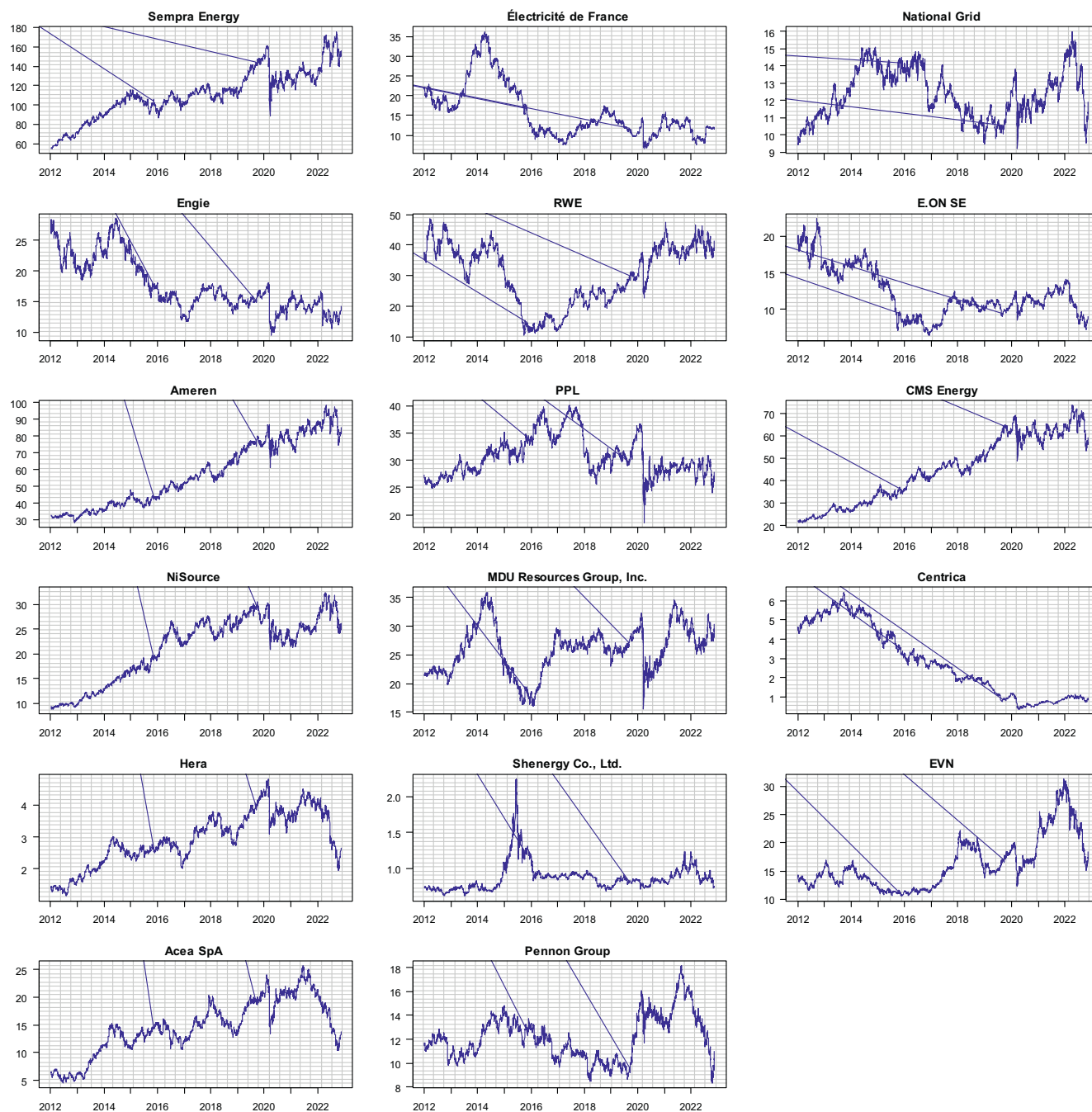


Fig. A3. Daily stock price trend of firms in the multiline utilities subsector

Note. The daily stock prices of companies in the multiline utilities are shown in this figure.

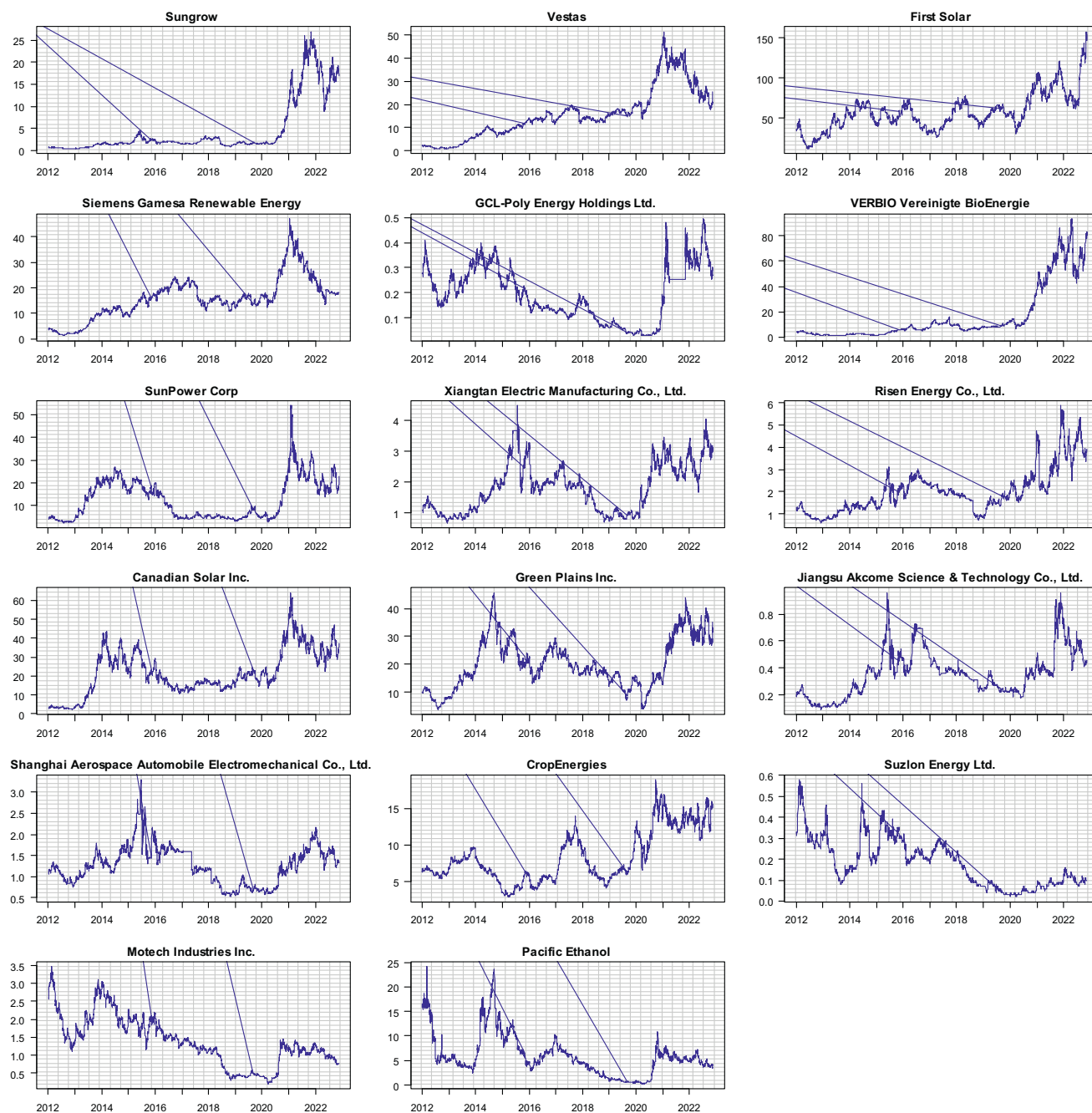


Fig. A4. Daily stock price trend of firms in the renewable energy subsector.

Note. The daily stock prices of companies in the renewable energy subsector are shown in this figure.

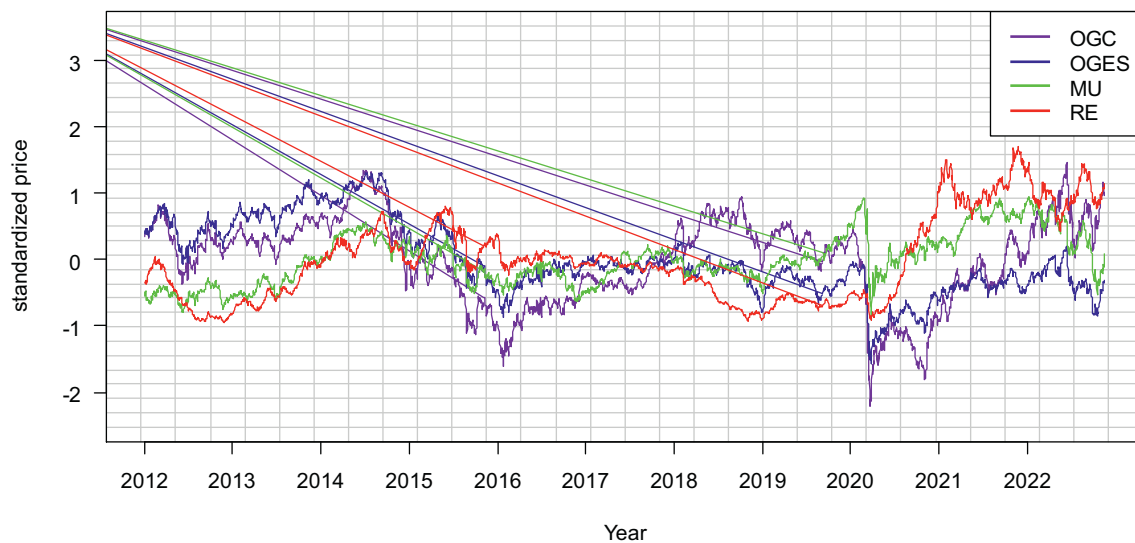


Fig. A5. Daily stock price trend of firms in the energy subsectors

Note. The daily stock prices (standardized) of companies in the energy sectors are shown in this figure, averaged by subsectors. OGC: oil and gas; OGES: oil and gas related equipment and services; MU: multiline utilities, and RE: renewable energy. OGC, OGES, MU, and RE are respectively indicated by purple, blue, green, and red.



Fig A6. Time-trend of global oil Price

Note. The dynamics of global oil price is shown in this figure.

Appendix B. Supplementary data

Supplementary data to this article can be found online at <https://doi.org/10.1016/j.eneco.2023.106882>.

References

- Abrell, J., Rausch, S., Streitberger, C., 2019. Buffering volatility: storage investments and technology-specific renewable energy support. *Energy Econ.* 84, 104463 <https://doi.org/10.1016/j.eneco.2019.07.023>.
- Adrian, T., Brunnermeier, M.K., 2016. CoVaR. *Am. Econ. Rev.* 106 (7), 1705–1741. <https://doi.org/10.1257/aer.20120555>.
- Agnolucci, P., De Lipsis, V., Arvanitopoulos, T., 2017. Modelling UK sub-sector industrial energy demand. *Energy Econ.* 67, 366–374. <https://doi.org/10.1016/j.eneco.2017.08.027>.
- Alolo, M., Azevedo, A., El Kalak, I., 2020. The effect of the feed-in-system policy on renewable energy investments: evidence from the EU countries. *Energy Econ.* 92, 104998 <https://doi.org/10.1016/j.eneco.2020.104998>.
- Antonakakis, N., Cunado, J., Filis, G., Gabauer, D., Perez de Gracia, F., 2018. Oil volatility, oil and gas firms and portfolio diversification. *Energy Econ.* 70, 499–515. <https://doi.org/10.1016/j.eneco.2018.01.023>.
- Bachmeier, L.J., Griffin, J.M., 2006. Testing for market integration: crude oil, coal, and natural gas. *Energy J.* 27 (2) <https://doi.org/10.5547/ISSN0195-6574-EJ-Vol27-No2-4>.
- Bekiros, S., Nguyen, D.K., Sandoval Junior, L., Uddin, G.S., 2017. Information diffusion, cluster formation and entropy-based network dynamics in equity and commodity markets. *Eur. J. Oper. Res.* 256 (3), 945–961. <https://doi.org/10.1016/j.ejor.2016.06.052>.
- Caporin, M., Fontini, F., Panzica, R., 2023. The systemic risk of US oil and natural gas companies. *Energy Econ.* 121, 106650 <https://doi.org/10.1016/J.ENECO.2023.106650>.
- Chakravorty, U., Roumasset, J., Tse, K., 1997. Endogenous substitution among energy resources and global warming. *J. Polit. Econ.* 105 (6), 1201–1234. <https://doi.org/10.1086/516390>.
- Chen, C.Y.H., Härdle, W.K., Okhrin, Y., 2019. Tail event driven networks of SIFIs. *J. Econ.* 208 (1), 282–298. <https://doi.org/10.1016/j.jeconom.2018.09.016>.
- Das, S.R., 2016. Matrix metrics: network-based systemic risk scoring. *J. Altern. Invest.* 18 (4), 33–51. <https://doi.org/10.3905/jai.2016.18.4.033>.
- Diebold, F.X., Yilmaz, K., 2014. On the network topology of variance decompositions: measuring the connectedness of financial firms. *J. Econ.* 182 (1), 119–134. <https://doi.org/10.1016/j.jeconom.2014.04.012>.
- Dogan, E., Altinoz, B., Madaleno, M., Taskin, D., 2020. The impact of renewable energy consumption to economic growth: a replication and extension of Inglesi-Lotz (2016). *Energy Econ.* 90, 104866 <https://doi.org/10.1016/j.eneco.2020.104866>.
- Domanski, D., Kearns, J., Lombardi Marco, J., Shin Hyun, S., 2015. Oil and debt. *BIS Quarterly Rev.* (March 2015).
- Du, L., He, Y., 2015. Extreme risk spillovers between crude oil and stock markets. *Energy Econ.* 51, 455–465. <https://doi.org/10.1016/j.eneco.2015.08.007>.
- Dutta, A., 2018. Implied volatility linkages between the U.S. and emerging equity markets: a note. *Glob. Financ. J.* 35, 138–146. <https://doi.org/10.1016/j.gfj.2017.09.002>.

- Elyasiani, E., Mansur, I., Odusami, B., 2011. Oil price shocks and industry stock returns. *Energy Econ.* 33 (5), 966–974. <https://doi.org/10.1016/j.eneco.2011.03.013>.
- Engle, R.F., 1982. Autoregressive conditional heteroscedasticity with estimates of the variance of United Kingdom inflation. *Econometrica* 50 (4), 987–1007. <https://doi.org/10.2307/1912773>.
- Ewing, B.T., Malik, F., Ozfidan, O., 2002. Volatility transmission in the oil and natural gas markets. *Energy Econ.* 24 (6), 525–538. [https://doi.org/10.1016/S0140-9883\(02\)00060-9](https://doi.org/10.1016/S0140-9883(02)00060-9).
- Fan, Y., Zhang, Y.J., Tsai, H.T., Wei, Y.M., 2008. Estimating ‘value at Risk’ of crude oil price and its spillover effect using the GED-GARCH approach. *Energy Econ.* 30 (6), 3156–3171. <https://doi.org/10.1016/j.eneco.2008.04.002>.
- Gong, B., 2018. Total-factor spillovers, similarities, and competitions in the petroleum industry. *Energy Econ.* 73, 228–238. <https://doi.org/10.1016/j.eneco.2018.04.036>.
- Hammoudeh, S., Dibooglu, S., Aleisa, E., 2004. Relationships among US oil prices and oil industry equity indices. *Int. Rev. Econ. Financ.* 13 (4), 427–453. [https://doi.org/10.1016/S1059-0560\(03\)00011-X](https://doi.org/10.1016/S1059-0560(03)00011-X).
- Hastie, T., Tibshirani, R., Wainwright, M., 2015. *Statistical Learning with Sparsity: The Lasso and Generalizations*. CRC press.
- Hautsch, N., Schaumburg, J., Schienle, M., 2015. Financial network systemic risk contributions. *Rev. Fin.* 19 (2), 685–738. <https://doi.org/10.1093/rof/rfu010>.
- Jarque, C.M., Bera, A.K., 1987. A test for normality of observations and regression residuals. *Int. Stat. Rev.* 55 (2), 163–172. <https://doi.org/10.2307/1403192>.
- Ji, Q., Fan, Y., 2015. Dynamic integration of world oil prices: a reinvestigation of globalisation vs. regionalisation. *Appl. Energy* 155, 171–180. <https://doi.org/10.1016/j.apenergy.2015.05.117>.
- Ji, Q., Fan, Y., 2016. How do China’s oil markets affect other commodity markets both domestically and internationally? *Financ. Res. Lett.* 19, 247–254. <https://doi.org/10.1016/j.frl.2016.08.009>.
- Jia, X., An, H., Sun, X., Huang, X., Wang, L., 2017. Evolution of world crude oil market integration and diversification: a wavelet-based complex network perspective. *Appl. Energy* 185, 1788–1798. <https://doi.org/10.1016/j.apenergy.2015.11.007>.
- Kerste, M., Gerritsen, M., Weda, J., Tieben, B., 2015. Systemic risk in the energy sector-is there need for financial regulation? *Energy Policy* 78, 22–30. <https://doi.org/10.1016/j.enpol.2014.12.018>.
- Li, J., Li, J., Zhu, X., 2020. Risk dependence between energy corporations: a text-based measurement approach. *Int. Rev. Econ. Financ.* 68, 33–46. <https://doi.org/10.1016/j.iref.2020.02.009>.
- Liu, X., An, H., Huang, S., Wen, S., 2017. The evolution of spillover effects between oil and stock markets across multi-scales using a wavelet-based GARCH-BEKK model. *Physica A: Stat. Mech. Appl.* 465, 374–383. <https://doi.org/10.1016/j.physa.2016.08.043>.
- Luo, X., Qin, S., 2017. Oil price uncertainty and Chinese stock returns: new evidence from the oil volatility index. *Financ. Res. Lett.* 20, 29–34. <https://doi.org/10.1016/j.frl.2016.08.005>.
- Madlener, R., Stagl, S., 2005. Sustainability-guided promotion of renewable electricity generation. *Ecol. Econ.* 53 (2), 147–167. <https://doi.org/10.1016/j.ecolecon.2004.12.016>.
- Masih, R., Peters, S., De Mello, L., 2011. Oil price volatility and stock price fluctuations in an emerging market: evidence from South Korea. *Energy Econ.* 33 (5), 975–986. <https://doi.org/10.1016/j.eneco.2011.03.015>.
- Mensi, W., Hammoudeh, S., Shahzad, S.J.H., Shahbaz, M., 2017. Modeling systemic risk and dependence structure between oil and stock markets using a variational mode decomposition-based copula method. *J. Bank. Financ.* 75, 258–279. <https://doi.org/10.1016/j.jbankfin.2016.11.017>.
- Miao, K., Phillips, P.C.B., Su, L., 2022. High-dimensional VARs with common factors. *J. Econ.* 233 (1), 155–183. <https://doi.org/10.1016/j.jeconom.2022.02.002>.
- Natalia, R., Jorge, M., U., & Diego, M., 2018. Financial risk network architecture of energy firms. *Appl. Energy* 215, 630–642. <https://doi.org/10.1016/j.apenergy.2018.02.060>.
- Natanolov, V., Alam, M.J., McKenzie, A.M., Van Huynenbroeck, G., 2011. Is there comovement of agricultural commodities futures prices and crude oil? *Energy Policy* 39 (9), 4971–4984. <https://doi.org/10.1016/j.enpol.2011.06.016>.
- Nations, U., 2018. The Paris agreement | UNFCCC [WWW document]. In: <https://unfccc.int/process-and-meetings/the-paris-agreement/the-paris-agreement>.
- Pesaran, M.H., Shin, Y., Smith, R.J., 2001. Bounds testing approaches to the analysis of level relationships. *J. Appl. Econ.* 16 (3), 289–326. <https://doi.org/10.1002/jae.616>.
- Pham, L., 2019. Do all clean energy stocks respond homogeneously to oil price? *Energy Econ.* 81, 355–379. <https://doi.org/10.1016/j.eneco.2019.04.010>.
- Reboredo, J.C., 2015. Is there dependence and systemic risk between oil and renewable energy stock prices? *Energy Econ.* 48, 32–45. <https://doi.org/10.1016/j.eneco.2014.12.009>.
- Sadorsky, P., 2001. Risk factors in stock returns of Canadian oil and gas companies. *Energy Econ.* 23 (1), 17–28. [https://doi.org/10.1016/S0140-9883\(00\)00072-4](https://doi.org/10.1016/S0140-9883(00)00072-4).
- Shahzad, S.J.H., Hernandez, J.A., Al-Yahyaee, K.H., Jammazi, R., 2018. Asymmetric risk spillovers between oil and agricultural commodities. *Energy Policy* 118, 182–198. <https://doi.org/10.1016/j.enpol.2018.03.074>.
- Silva, W., Kimura, H., Sobreiro, V.A., 2017. An analysis of the literature on systemic financial risk: a survey. *J. Financ. Stab.* 28, 91–114. <https://doi.org/10.1016/j.jfs.2016.12.004>.
- Singh, V.K., Kumar, P., Nishant, S., 2019. Global connectedness of MSCI energy equity indices: a system-wide network approach. *Energy Econ.* 84, 104477. <https://doi.org/10.1016/j.eneco.2019.104477>.
- Steffen, B., 2020. Estimating the cost of capital for renewable energy projects. *Energy Econ.* 88, 104783. <https://doi.org/10.1016/j.eneco.2020.104783>.
- Wen, X., Guo, Y., Wei, Y., Huang, D., 2014. How do the stock prices of new energy and fossil fuel companies correlate? Evidence from China. *Energy Econ.* 41, 63–75. <https://doi.org/10.1016/j.eneco.2013.10.018>.
- Zhu, B., Lin, R., Liu, J., 2020. Magnitude and persistence of extreme risk spillovers in the global energy market: a high-dimensional left-tail interdependence perspective. *Energy Econ.* 89, 104761. <https://doi.org/10.1016/j.eneco.2020.104761>.